ISSN 1560-3547, Regular and Chaotic Dynamics, 2019, Vol. 24, No. 5, pp. 560–582. © Pleiades Publishing, Ltd., 2019.

Different Models of Rolling for a Robot Ball on a Plane as a Generalization of the Chaplygin Ball Problem

Ivan A. Bizyaev[1, 2*], Alexey V. Borisov[3], and Ivan S. Mamaev[1, 4***]**

[1] *Moscow Institute of Physics and Technology, Institutskii per. 9, Dolgoprudnyi, 141700 Russia*

[2] *Center for Technologies in Robotics and Mechatronics Components, Innopolis University, ul. Universitetskaya 1, Innopolis, 420500 Russia*

[3] *Udmurt State University, ul. Universitetskaya 1, Izhevsk, 426034 Russia*

[4] *Institute of Mathematics and Mechanics of the Ural Branch of RAS, ul. S. Kovalevskoi 16, Ekaterinburg, 620990 Russia*

Received July 08, 2019; revised August 20, 2019; accepted August 26, 2019

Abstract—This paper addresses the problem of the rolling of a spherical shell with a frame rotating inside, on which rotors are fastened. It is assumed that the center of mass of the entire system is at the geometric center of the shell.

For the rubber rolling model and the classical rolling model it is shown that, if the angular velocities of rotation of the frame and the rotors are constant, then there exists a noninertial coordinate system (attached to the frame) in which the equations of motion do not depend explicitly on time. The resulting equations of motion preserve an analog of the angular momentum vector and are similar in form to the equations for the Chaplygin ball. Thus, the problem reduces to investigating a two-dimensional Poincaré map.

The case of the rubber rolling model is analyzed in detail. Numerical investigation of its Poincaré map shows the existence of chaotic trajectories, including those associated with a strange attractor. In addition, an analysis is made of the case of motion from rest, in which the problem reduces to investigating the vector field on the sphere S^2.

MSC2010 numbers: 37J60, 37C10

DOI: 10.1134/S1560354719050071

Keywords: nonholonomic mechanics, Chaplygin ball, rolling without slipping and spinning, strange attractor, straight-line motion, stability, limit cycle, balanced beaver-ball

Contents

*E-mail: bizaev_90@mail.ru

**E-mail: borisov@rcd.ru

***E-mail: mamaev@rcd.ru

1. INTRODUCTION

1. This paper is dedicated to the 150th birthday of renowned Russian mechanical engineer and mathematician S. A. Chaplygin. A conference[1)] has been held in honor of this event in the Russian city of Cheboksary. We note that S. A. Chaplygin made a considerable contribution to various fields of science, including aeromechanics, fluid dynamics, nonholonomic mechanics, and rigid body dynamics. His biography is set forth in detail in the book by Golubev [39]. In addition, since 2002 the journal *Regular and Chaotic Dynamics* has been publishing English translations of S. A. Chaplygin's papers devoted to nonholonomic mechanics [29, 30, 30] and the dynamics of vortex structures [32, 33].

In this paper we investigate a mechanical system with nonholonomic constraints. Therefore, we consider briefly the contribution of Chaplygin to this area. Since the work of Hertz, nonholonomic mechanics has been concerned mainly with the development of various principles and forms of equations (the history of nonholonomic mechanics is reviewed in detail in [24, 25]). The contribution of Chaplygin is that, in addition to the development of a new form of equations and the theory of the last multiplier, he posed a number of insightful problems, which continue to be of much current interest and are essential to mechanics and mobile robotics.

Fig. 1. Sergei A. Chaplygin (1869–1942).

We recall the standard nonholonomic systems which were introduced in the papers by S. A. Chaplygin: the Chaplygin ball, the Chaplygin sleigh, and the Chaplygin top. We also mention an unpublished paper by Chaplygin on the nonholonomic system of two coupled bodies (a ball with a pendulum inside), which was discussed in [16].

The ideas of S. A. Chaplygin owe their further development in nonholonomic mechanics primarily to the work of V.V.Kozlov [44], in which various generalizations of Chaplygin's problems are discussed. In addition, his work highlights the key role of various tensor invariants in analyzing the behavior of nonholonomic systems, in particular, it shows an obstruction to the existence of an invariant measure. Later, these ideas were also developed in [20, 27, 28], which formed the general idea of the hierarchy of dynamical behavior of nonholonomic systems.

2. Let us consider in more detail the Chaplygin ball problem. We recall that the Chaplygin ball is a spherical rigid body in which the principal moments of inertia are different and the center of mass is at the geometric center. For the first time this problem was explicitly integrated by S. A. Chaplygin [29] in 1903. In this case, the equations of motion have an invariant measure, preserve energy and the angular momentum vector referred to the axes of a fixed coordinate system. This case is similar to the Euler case in rigid body dynamics and can be exactly reduced to it if the angular momentum lies in the direction perpendicular to the horizontal plane [14, 29].

[1)] http://umu.chuvsu.ru/chaplygin2019

However, in contrast to the Euler case, (reduced) equations of motion are represented in Hamiltonian form only after rescaling time [22]. An explicit representation in conformally Hamiltonian form is presented in [23], and some justification of the found representation is discussed in [2]. An analysis of trajectories of the point of contact of the Chaplygin ball on a plane is presented in [13].

3. In connection with the development of the methods of nonholonomic mechanics and possible applications of rolling balls to robotics, various versions of the Chaplygin ball rolling problem are considered:

— addition of *gyrostatic momentum* [48] and *the Brun field* [44];

— rolling in a *spherical suspension* (BMF system) [9, 10], a *ball suspension* [14, 37] and *on a uniformly rotating plane* [3, 11, 35, 51];

— addition of *a fluid-filled cavity* to the ball [21].

We also highlight a new spectrum of problems which involve considering another nonholonomic model. In addition to assuming that the velocity of the point of contact is zero, this model assumes that the projection of the angular velocity onto the normal to the plane is also zero (i.e., there is no spinning). In [34] it is proposed to implement this model by coating the rolling body with sufficiently soft rubber (see also [42]). This is why it is also called the *rubber rolling model*.

Within the rubber model the Chaplygin ball rolling problem is integrable and is addressed in [19, 27]. It has turned out that in the case of the Chaplygin ball there exists an interrelation between the rubber rolling model and the standard (classical) model of rolling without slipping with the possibility of spinning: the trajectories of the reduced system for the Chaplygin ball turn out to be transversal (to each other) windings of the same tori [8, 52].

4. Of particularly great interest from the viewpoint of control theory and various applications [12] are problems of the rolling of a ball with periodically varying mass distribution, which is caused by the control mechanism placed inside the ball [41, 43, 49]. The qualitative analysis of such systems is complicated by the fact that they reduce to investigating a Poincaré map, which defies visualization (since its dimension is greater than three). Moreover, the reduced equations of motion explicitly depend on time, which makes the stability analysis of particular motions difficult.

One of the simplest examples of such systems is the (toy) beaver ball[2)] (see Fig. 2). It is a spherical shell inside which a rigid body (rotor, frame) rotates with constant angular velocity about the axis passing through the geometric center of the sphere. The body is fastened in such a way that its center of mass does not lie on the axis of rotation. As a result, the center of mass of the entire system is displaced relative to the geometric center of the shell and executes periodic motion. In [41] this influence of the rigid body is modeled using a material point which moves in a circle, and the analysis of the equations of motion thus obtained is confined to numerically constructing the trajectory of the point of contact and the time dependence of the angular velocity of the ball for fixed initial conditions and parameters.

Fig. 2. Beaver ball in dismantled form.

It has recently been shown [4–6, 43] that nonholonomic systems with periodically varying mass distribution may exhibit motions where the velocity of the carrying body increases indefinitely. In contrast to Hamiltonian systems (see, e. g., [47]), the indefinite increase in the velocity is characteristic of systems that reduce to a two-dimensional map which is no longer area-preserving.

[2)] The use of the word *beaver* is due to the fact that commercial variants have a furry toy fastened on the outer side of the sphere.

5. In this paper, we consider the problem of the rolling of a dynamically symmetric spherical shell with a frame (rigid body) which rotates along its symmetry axis and on which rotors (gyrostats) are fastened. It is assumed that the center of mass of the entire system is at the geometric center of the ball. This case arises, for example, if one places the rigid body inside the shell of the beaver ball in such a way that its center of mass is at the geometric center of the shell (balanced beaver ball).

Generally speaking, the analysis of dynamical equations of an (unbalanced) beaver ball is complicated by the large dimension of the Poincaré map. For the system under consideration, the problem is reduced, by using additional integrals, to investigating of a two-dimensional Poincaré map. We present the main results obtained in this study:

— Equations of motion are obtained which describe the rolling without slipping (for the classical rolling model and the rubber rolling model) of a robot with a spherical shell. In the case of constant velocity of rotation of the shell relative to the frame (capsule), a representation of the equations of motion in the form of an autonomous system is found which is a generalization of the nonholonomic system in the Chaplygin ball problem (see Section 2). In this case, however, these equations have no continuous invariant measure and no energy integral.

— Conservation laws (first integrals) are found and it is shown that on the corresponding integral surface (which turns out to be three-dimensional) the analysis of the reduced system can be carried out using a two-dimensional Poincaré map (see Section 3).

— A qualitative analysis for the rubber rolling model is carried out in the case of motion of the system from rest. In particular, a stability analysis is made of partial solutions that correspond to the fixed points of the reduced system. The asymptotic nature of the behavior of the system in a neighborhood of these solutions suggests that that there is no continuous invariant measure. This is indicative of a considerable difference of this system from the Chaplygin ball problem and its various generalizations (see Section 4).

— Partial solutions are found for which the internal frame (capsule) remains fixed relative to the supporting surface, and conditions for their stability (gyroscopic stabilization) are analyzed (see Section 5.1).

— It is shown that at certain parameter values the system may exhibit irregular (chaotic) behavior. In this case, a strange attractor arises in the phase space of the reduced system (see Section 5.2).

The beaver ball is of interest to children, since it exhibits interesting dynamical behavior — it moves chaotically on the plane and behaves particularly strangely when colliding with obstacles. For the system considered in this paper, problems of chaotic behavior in the reduced phase space and of the behavior of the point of contact are only touched upon. Yet these problems, which are undoubtedly of interest, require a more detailed investigation of the resulting system.

2. EQUATIONS OF MOTION

Consider a system moving on a horizontal plane and consisting of several bodies (see Fig. 3):

1) a dynamically symmetric *spherical shell* in which the center of mass is at the geometric center;

2) a *frame,*[3)] a rigid body with an arbitrary mass distribution, which is fastened inside the shell by means of cylindrical hinges. The frame is able to rotate relative to the shell with a given angular velocity $\boldsymbol{\Omega}(t)$;

3) n dynamically symmetric rigid bodies (*rotors*) which are fastened on the frame.

We assume that the frame and the rotors are located inside the spherical shell in such a way that *the center of mass of the entire system is at the geometric center of the shell*, that is, we consider a balanced case.

[3)] As a rule, it is the frame that is of the greatest technical importance in mobile devices, since devices for observations, life-support capsules etc. can be connected with it. Therefore, its stabilization relative to the fixed coordinate system is a high-priority problem.

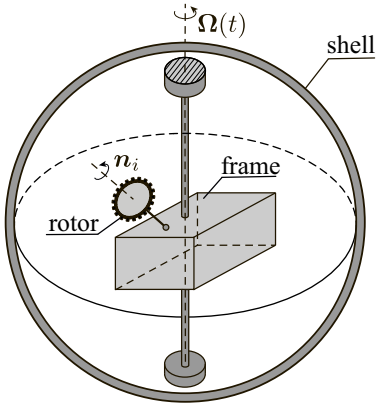

Fig. 3. Structure of the system for one rotor ($n = 1$).

Suppose that the frame and the rotors execute the following motion relative to the shell:

— the frame rotates with angular velocity $\boldsymbol{\Omega}(t)$, given as a function of time, about the axis of dynamical symmetry of the shell. If the shell is homogeneous, then any straight line passing through the geometric center of the shell can be chosen as the axis of rotation of the frame;

— the rotors rotate (relative to the frame) with angular velocity $\dot{\phi}_i(t)$, given as a function of time, about its axis of dynamical symmetry $\boldsymbol{n}_i$.

We define two coordinate systems (see Fig. 4):

— an *inertial* coordinate system $OXYZ$ with origin at some point of the plane and with the axis OZ perpendicular to it.

— a *noninertial* coordinate system $Cx_1x_2x_3$, which is attached to the frame, so that the origin C coincides with the center of mass of the system.

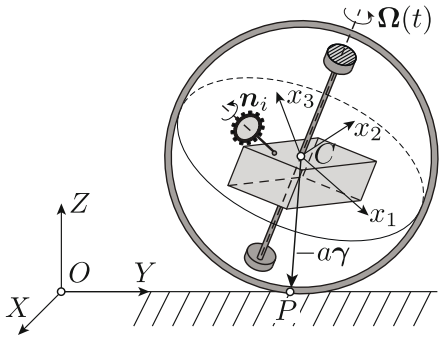

Fig. 4. The system on the plane.

A distinctive feature of this system is the fact that the mass distribution remains constant in the coordinate system $Cx_1x_2x_3$. This is due to the fact that the rotors and the shell in this system rotate in a prescribed manner about their symmetry axes (in contrast to the coordinate system attached to the shell).

Configuration space. Let $\boldsymbol{R}_C = (X_c, Y_c, Z_c)$ be the coordinates of the center of mass of the system in the inertial coordinate system $OXYZ$ and let $\mathbf{S}$ be the matrix of rotation of the fixed axes relative to the coordinate system attached to the frame $Cx_1x_2x_3$.

Let us parameterize $\mathbf{S}$ by $\boldsymbol{\alpha}$, $\boldsymbol{\beta}$ and $\boldsymbol{\gamma}$, the unit vectors of the inertial coordinate system referred to the axes $Cx_1x_2x_3$:

$$\mathbf{S} = \begin{pmatrix} \alpha_1 & \beta_1 & \gamma_1 \\ \alpha_2 & \beta_2 & \gamma_2 \\ \alpha_3 & \beta_3 & \gamma_3 \end{pmatrix} \in SO(3),$$

where the unit vector $\boldsymbol{\gamma}$ defines the normal to the plane, i.e., it is directed along the axis OZ.

Remark 1. In this case, obvious geometric relations expressing the condition of orthogonality of the matrix $\mathbf{S}$ are satisfied:

$$(\boldsymbol{\alpha},\boldsymbol{\beta}) = (\boldsymbol{\beta},\boldsymbol{\gamma}) = (\boldsymbol{\gamma},\boldsymbol{\alpha}) = 0,$$
$$\boldsymbol{\alpha}^2 = \boldsymbol{\beta}^2 = \boldsymbol{\gamma}^2 = 1.$$

Since the motion of the shell and the rotor relative to the frame is defined at any instant of time, the pair $\boldsymbol{R}_C$, $\boldsymbol{S}$ uniquely defines the configuration of the system. Thus,

$$\mathscr{N} = \{\boldsymbol{R}_C, \boldsymbol{S}\} \approx \mathbb{R}^3 \times SO(3)$$

is the configuration space of this system.

Remark 2. Here and in what follows, we denote vectors by bold italic $\boldsymbol{a},\boldsymbol{b},\ldots$, and write their scalar and vector product as $(\boldsymbol{a},\boldsymbol{b})$ and $\boldsymbol{a}\times\boldsymbol{b}$, respectively. The sign $\widehat{\ }$ above the vector denotes the skew-symmetric matrix $\widehat{\boldsymbol{a}} = \varepsilon_{ijk}a_k$, where ε_{ijk} is the Levi-Civita symbol. The sign $\otimes$ denotes a tensor product, i. e., in matrix form $\boldsymbol{a}\otimes\boldsymbol{b} = ||a_ib_j||$. Boldface upright font is used to denote the matrices: $\mathbf{A},\mathbf{B},\ldots$.

Quasi-velocities. We parameterize the tangent space $T\mathscr{N}$ by the velocity of the center of mass of the system, $\boldsymbol{v} = (v_1, v_2, v_3)$, and by the angular velocity of the frame, $\boldsymbol{\omega} = (\omega_1, \omega_2, \omega_3)$, which are referred to the moving axes $Cx_1x_2x_3$. They are expressed in terms of configuration variables and their derivatives as follows (see [17] for details):

$$\widehat{\boldsymbol{\omega}} = \dot{\mathbf{S}}\mathbf{S}^T, \quad \boldsymbol{v} = \mathbf{S}\dot{\boldsymbol{R}}_C,$$
$$\widehat{\boldsymbol{\omega}} = \begin{pmatrix} 0 & \omega_3 & -\omega_2 \\ -\omega_3 & 0 & \omega_1 \\ \omega_2 & -\omega_1 & 0 \end{pmatrix}.$$

Here and in what follows (unless otherwise specified), all vectors are referred to the moving axes $Cx_1x_2x_3$.

Models of rolling and constraint equations. Two nonholonomic models of a shell rolling on a plane are possible:

1. The model of rolling without slipping (*classical rolling model*), in which the velocity at the contact point of the shell is zero:

$$\boldsymbol{f} = \boldsymbol{v} + a\boldsymbol{\gamma}\times\big(\boldsymbol{\omega} - \boldsymbol{\Omega}(t)\big) = 0, \tag{2.1}$$

   where a is the radius of the spherical shell.

2. The model of rolling without slipping and spinning (*rubber rolling model*), which, in addition to assuming zero velocity of the point of contact, assumes that there is no spinning of the shell relative to $\boldsymbol{\gamma}$, the normal to the plane at the point of contact P:

$$f_0 = (\boldsymbol{\omega} - \boldsymbol{\Omega}(t), \boldsymbol{\gamma}) = 0. \tag{2.2}$$

   As a rule, this model is called the rubber rolling model [27, 34] to emphasize that, by coating the body with rubber, one can ensure a proper contact with the plane.

Thus, in the coordinate system $Cx_1x_2x_3$ nonholonomic constraints are given by relations that are inhomogeneous in the velocities $\boldsymbol{v}$ and $\boldsymbol{\omega}$.

Kinetic energy. The kinetic energy in the coordinate system $Cx_1x_2x_3$ can be represented as

$$T = \frac{1}{2}m\boldsymbol{v}^2 + \frac{1}{2}(\boldsymbol{\omega}, \mathbf{I}\boldsymbol{\omega}) + (\boldsymbol{k}(t), \boldsymbol{\omega}),$$

where m and $\mathbf{I}$ are, respectively, the mass and the tensor of inertia of the system, and $\boldsymbol{k}(t)$ is the vector of the total gyrostatic momentum of the rotors and the frame, which is expressed in terms of their angular velocities (see relations (A.3)):

$$\boldsymbol{k}(t) = \sum_{i=1}^{n} j_i\dot{\phi}_i(t)\boldsymbol{n}_i - J_{\mathrm{s}}\boldsymbol{\Omega}(t),$$

where J_{s} and j_i are the moments of inertia of the shell and the ith rotor, respectively.

We direct the axes of the coordinate system $Cx_1x_2x_3$ along the principal axes of inertia of the system, thus, $\mathbf{I} = \operatorname{diag}(I_1, I_2, I_3)$ is a diagonal matrix. A derivation of relations for nonholonomic constraints and the kinetic energy of the system is presented in Appendix A.

Equations of motion. In the general case, we represent the equations of motion in the form of Poincaré – Suslov equations (for details, see [18, 38]):

$$\begin{gathered}\frac{d}{dt}\left(\frac{\partial T}{\partial \boldsymbol{\omega}}\right) + \boldsymbol{\omega} \times \frac{\partial T}{\partial \boldsymbol{\omega}} + \boldsymbol{v} \times \frac{\partial T}{\partial \boldsymbol{v}} + \boldsymbol{\gamma} \times \frac{\partial T}{\partial \boldsymbol{\gamma}} = \sum_{i=1}^{3} \lambda_i \frac{\partial f_i}{\partial \boldsymbol{\omega}} + \lambda_0 \frac{\partial f_0}{\partial \boldsymbol{\omega}},\\ \frac{d}{dt}\left(\frac{\partial T}{\partial \boldsymbol{v}}\right) + \boldsymbol{\omega} \times \frac{\partial T}{\partial \boldsymbol{v}} = \sum_{i=1}^{3} \lambda_i \frac{\partial f_i}{\partial \boldsymbol{v}} + \lambda_0 \frac{\partial f_0}{\partial \boldsymbol{v}},\end{gathered} \tag{2.3}$$

where $\boldsymbol{\lambda} = (\lambda_1, \lambda_2, \lambda_3)$ and λ_0 are the undetermined multipliers defining the reaction of the constraints (2.1) and (2.2), respectively.

Remark 3. The center of mass of the entire system coincides with the geometric center, therefore, the system of equations (2.3) contains no terms with potential of the gravitational field (since $U = \text{const}$).

Differentiating the constraint (2.1), we find from the last equation of (2.3):

$$\boldsymbol{\lambda} = -ma\boldsymbol{\gamma} \times \big(\dot{\boldsymbol{\omega}} - \dot{\boldsymbol{\Omega}}(t)\big) - ma\dot{\boldsymbol{\gamma}} \times \big(\boldsymbol{\omega} - \boldsymbol{\Omega}(t)\big) - ma\boldsymbol{\omega} \times \big(\boldsymbol{\gamma} \times (\boldsymbol{\omega} - \boldsymbol{\Omega}(t))\big).$$

Substituting $\boldsymbol{\lambda}$ thus found into the first equation of (2.3) and writing a kinematic relation for the normal vector $\boldsymbol{\gamma}$, we obtain

$$\begin{aligned}\tilde{\mathbf{I}}\dot{\boldsymbol{\omega}} &= \big(\tilde{\mathbf{I}}\boldsymbol{\omega} + \boldsymbol{k}(t)\big) \times \boldsymbol{\omega} + ma^2\big(\boldsymbol{\omega} - \boldsymbol{\Omega}(t), \boldsymbol{\gamma}\big)\boldsymbol{\gamma} \times \boldsymbol{\omega} + \lambda_0\boldsymbol{\gamma}\\ &\quad + ma^2(\boldsymbol{\omega}, \boldsymbol{\gamma})\boldsymbol{\gamma} \times \boldsymbol{\Omega}(t) + ma^2\boldsymbol{\gamma} \times \big(\dot{\boldsymbol{\Omega}}(t) \times \boldsymbol{\gamma}\big) - \dot{\boldsymbol{k}}(t),\\ \tilde{\mathbf{I}} &= \mathbf{I} + ma^2(\boldsymbol{\gamma}^2 - \boldsymbol{\gamma} \otimes \boldsymbol{\gamma}),\\ \dot{\boldsymbol{\gamma}} &= \boldsymbol{\gamma} \times \boldsymbol{\omega}.\end{aligned} \tag{2.4}$$

where $\tilde{\mathbf{I}}$ is the tensor of inertia of the system relative to the point of contact P.

In order to obtain equations of motion in the classical rolling model in the system (2.4)*, we need to set* $\lambda_0 = 0$*, and in the case of the rubber rolling model* λ_0 *is defined from the constraint* (2.2)*.*

Differentiating the constraint (2.2) with respect to time, we obtain

$$(\tilde{\mathbf{I}}\dot{\boldsymbol{\omega}}, \tilde{\mathbf{I}}^{-1}\boldsymbol{\gamma}) - (\boldsymbol{\Omega}(t), \boldsymbol{\gamma} \times \boldsymbol{\omega}) + (\dot{\boldsymbol{\Omega}}(t), \boldsymbol{\gamma}) = 0.$$

From this equation, taking (2.4) into account, we find the undetermined multiplier λ_0 as a function of the angular velocity $\boldsymbol{\omega}$ and of the normal $\boldsymbol{\gamma}$:

$$\begin{aligned}\lambda_0 &= -\frac{\Big(\tilde{\mathbf{I}}^{-1}\boldsymbol{\gamma}, \big(\tilde{\mathbf{I}}\boldsymbol{\omega} + \boldsymbol{k}(t)\big) \times \boldsymbol{\omega} + ma^2\big(\boldsymbol{\omega} - \boldsymbol{\Omega}(t), \boldsymbol{\gamma}\big)\boldsymbol{\gamma} \times \boldsymbol{\omega} + \boldsymbol{W}\Big)}{(\tilde{\mathbf{I}}^{-1}\boldsymbol{\gamma}, \boldsymbol{\gamma})}\\ &\quad + \frac{(\boldsymbol{\Omega}(t), \boldsymbol{\gamma} \times \boldsymbol{\omega}) + (\dot{\boldsymbol{\Omega}}(t), \boldsymbol{\gamma})}{(\tilde{\mathbf{I}}^{-1}\boldsymbol{\gamma}, \boldsymbol{\gamma})},\\ \boldsymbol{W} &= ma^2(\boldsymbol{\omega}, \boldsymbol{\gamma})\boldsymbol{\gamma} \times \boldsymbol{\Omega}(t) + ma^2\boldsymbol{\gamma} \times \big(\dot{\boldsymbol{\Omega}}(t) \times \boldsymbol{\gamma}\big) - \dot{\boldsymbol{k}}(t).\end{aligned} \tag{2.5}$$

We see that Eqs. (2.4) are closed relative to the variables $\boldsymbol{\omega}$, $\boldsymbol{\gamma}$ and form a reduced system.

Reconstruction of dynamics. From the known functions $\boldsymbol{\omega}(t)$ and $\boldsymbol{\gamma}(t)$ the orientation of the frame is described by the following system of equations:

$$\dot{\boldsymbol{\alpha}} = \boldsymbol{\alpha} \times \boldsymbol{\omega}, \quad \dot{\boldsymbol{\beta}} = \boldsymbol{\beta} \times \boldsymbol{\omega}. \tag{2.6}$$

The equations of motion for the coordinates of the contact point $\boldsymbol{R}_P = (X, Y, 0)$ of the shell in the fixed coordinate system $OXYZ$ have the form

$$\dot{X} = a\big(\boldsymbol{\beta}, \boldsymbol{\omega} - \boldsymbol{\Omega}(t)\big), \quad \dot{Y} = -a\big(\boldsymbol{\alpha}, \boldsymbol{\omega} - \boldsymbol{\Omega}(t)\big). \tag{2.7}$$

In the noninertial coordinate system $Cx_1x_2x_3$ (attached to the frame) the equations of motion (2.4), (2.6) and (2.7) have a simpler form than the equations in the coordinate system attached to the shell, which makes them amenable to a detailed qualitative analysis.

Below, we will consider separately the case of the rubber rolling and that of the classical rolling of the ball, since the conservation laws for them are different.

Remark 4. In this case, the symmetry group of the entire system is the group of motions of the plane $SE(2)$. We see that the components of the vectors $\boldsymbol{\omega}$ and $\boldsymbol{\gamma}$ are its invariants. Consequently, choosing the suitable coordinate system $Cx_1x_2x_3$, we have in fact performed a reduction by symmetries.

3. CONSERVATION LAWS

3.1. Rolling of the Shell Without Slipping and Spinning (Rubber Model)

Let us define the angular momentum:

$$\boldsymbol{M} = \boldsymbol{\gamma} \times \big(\tilde{\mathbf{I}}\boldsymbol{\omega} - \boldsymbol{K}(t)\big), \quad \boldsymbol{K}(t) = \boldsymbol{k}(t) - ma^2\boldsymbol{\Omega}(t), \tag{3.1}$$

which lies in the horizontal plane OXY:

$$(\boldsymbol{M}, \boldsymbol{\gamma}) = 0.$$

The equations of motion for $\boldsymbol{M}$ and $\boldsymbol{\gamma}$, taking the constraint (2.2) into account, can be represented as

$$\begin{gathered} \dot{\boldsymbol{M}} = \boldsymbol{M} \times \boldsymbol{\omega}, \quad \dot{\boldsymbol{\gamma}} = \boldsymbol{\gamma} \times \boldsymbol{\omega}, \\ \boldsymbol{\omega} = \mathbf{A}\left(\frac{\boldsymbol{M} \times \mathbf{A}\boldsymbol{\gamma}}{(\mathbf{A}\boldsymbol{\gamma}, \boldsymbol{\gamma})} - \boldsymbol{K}(t) + Z\boldsymbol{\gamma}\right), \quad Z = \frac{(\boldsymbol{\Omega}(t) + \mathbf{A}\boldsymbol{K}(t), \boldsymbol{\gamma})}{(\mathbf{A}\boldsymbol{\gamma}, \boldsymbol{\gamma})}, \end{gathered} \tag{3.2}$$

where $\mathbf{A} = \operatorname{diag}(a_1, a_2, a_3) = (\mathbf{I} + ma^2\mathbf{E})^{-1}$ is the diagonal matrix.

As can be seen, the angular momentum $\boldsymbol{M}$ is constant in the fixed coordinate system $OXYZ$, and hence the reduced system (3.2) possesses the following integrals of motion:

$$F_0 = \boldsymbol{\gamma}^2, \quad F_1 = (\boldsymbol{M}, \boldsymbol{\gamma}), \quad F_2 = \boldsymbol{M}^2,$$

and, according to the definition of $\boldsymbol{M}$ and $\boldsymbol{\gamma}$, we obtain $F_0 = 1$, $F_1 = 0$.

Now suppose that the angular velocity of the frame and the generalized gyrostatic momentum *do not depend explicitly on time*:

$$\boldsymbol{\Omega} = \text{const}, \quad \boldsymbol{K} = \text{const}.$$

Then the problem reduces to investigating the autonomous system of Eqs. (3.2), which describes the flow on the three-dimensional manifold parameterized by the value of the integral $F_2 = f =$ const:

$$\mathscr{M}^3_f = \{(\boldsymbol{M}, \boldsymbol{\gamma}) \mid \boldsymbol{\gamma}^2 = 1, (\boldsymbol{M}, \boldsymbol{\gamma}) = 0, \boldsymbol{M}^2 = f\},$$

which is a bundle of unit tangent vectors [40].

Remark 5. If $\boldsymbol{\Omega} \neq 0$, then the nonholonomic constraints (2.1) and (2.2) are inhomogeneous in the velocities. As is well known [26, 35], the equations of motion (3.2) generally have no energy integral for such systems. Nevertheless, if $\mathbf{A}$ is an axisymmetric matrix and the vectors $\boldsymbol{\Omega}$ and $\boldsymbol{K}$ are directed along its symmetry axis, then the system (3.2) describes the rolling of a balanced *Routh sphere* with a rotor. In this case, the system (3.2) has an energy integral and an invariant measure (i. e., it is integrable by quadratures [20, 45]) in the rubber and the classical rolling model. We will not consider this case in what follows.

For the system (3.2) to be integrable by the Euler – Jacobi theorem, we need an additional integral and an invariant measure. Below it will be shown that in the general case the system (3.2) has chaotic trajectories, which suggests that it has no analytic integrals. In addition, simple and strange attractors will be found, and so, in the general case, there is no invariant measure with continuous density.

3.2. Rolling of the Shell Without Slipping (Classical Model)

It turns out that, in the case of the classical rolling model there also exists angular momentum $\boldsymbol{M}$, which is constant in the fixed coordinate system $OXYZ$. We represent it in the following form:

$$\boldsymbol{M} = \tilde{\mathbf{I}}\boldsymbol{\omega} + \boldsymbol{K}(t) - d(\boldsymbol{\Omega}(t), \boldsymbol{\gamma})\boldsymbol{\gamma}, \quad \boldsymbol{K}(t) = \boldsymbol{k}(t) - d\boldsymbol{\Omega}(t), \ d = ma^2.$$

The reduced equations of motion for $\boldsymbol{M}$ and $\boldsymbol{\gamma}$ have the form

$$\begin{gathered} \dot{\boldsymbol{M}} = \boldsymbol{M} \times \boldsymbol{\omega}, \quad \dot{\boldsymbol{\gamma}} = \boldsymbol{\gamma} \times \boldsymbol{\omega}, \\ \boldsymbol{\omega} = \mathbf{A}(\boldsymbol{M} - \boldsymbol{K}(t) + Z\boldsymbol{\gamma}), \quad Z = \frac{\big(\mathbf{A}(\boldsymbol{M} - \boldsymbol{K}(t)) - \boldsymbol{\Omega}, \boldsymbol{\gamma}\big)}{d^{-1} - (\mathbf{A}\boldsymbol{\gamma}, \boldsymbol{\gamma})}, \end{gathered} \tag{3.3}$$

where $\mathbf{A} = (\mathbf{I} + ma^2\mathbf{E})^{-1}$ is the diagonal matrix.

Thus, the system possesses the following integrals of motion:

$$F_0 = \boldsymbol{\gamma}^2, \quad F_1 = (\boldsymbol{M}, \boldsymbol{\gamma}), \quad F_2 = \boldsymbol{M}^2,$$

where $F_0 = 1$ and, in contrast to the rubber model, in the general case one has $F_1 \neq 0$.

If one assumes the angular velocity of the frame and the gyrostatic momentum to be constant ($\boldsymbol{\Omega} = \text{const}$, $\boldsymbol{K} = \text{const}$), then, as in the rubber rolling model, the problem reduces to investigating the autonomous system of equations (3.2), which describes the flow on the three-dimensional manifold parameterized by the values of the integrals $F_1 = c = \text{const}$ and $F_2 = f = \text{const}$:

$$\mathscr{M}^3_{c,f} = \{(\boldsymbol{M}, \boldsymbol{\gamma}) \mid \boldsymbol{\gamma}^2 = 1, (\boldsymbol{M}, \boldsymbol{\gamma}) = c, \boldsymbol{M}^2 = f\}.$$

For the system (3.3) to be integrable by the Euler – Jacobi theorem, we need an additional integral and an invariant measure.

3.3. Reconstruction for Fixed Values of First Integrals

In this case, by choosing the orientation of the axes of the fixed coordinate system one can eliminate the equations of motion (2.6) for the unit vectors $\boldsymbol{\alpha}$ and $\boldsymbol{\beta}$ (i. e., perform reduction). We describe this procedure in more detail.

Let $\boldsymbol{M} \neq 0$ and $\boldsymbol{M} \nparallel \boldsymbol{\gamma}$ (the latter condition is automatically satisfied for the rubber rolling model, since $(\boldsymbol{M}, \boldsymbol{\gamma}) = 0$). Then on the fixed level set of the first integrals $\boldsymbol{M}^2 = f$, $(\boldsymbol{M}, \boldsymbol{\gamma}) = c$ we choose the unit vectors $\boldsymbol{\alpha}$ and $\boldsymbol{\beta}$ in the form

$$\boldsymbol{\alpha} = -\frac{\boldsymbol{M} - c\boldsymbol{\gamma}}{\sqrt{f - c^2}}, \quad \boldsymbol{\beta} = \frac{\boldsymbol{M} \times \boldsymbol{\gamma}}{\sqrt{f - c^2}}.$$

This yields equations for the trajectory of the point of contact in the form

$$\dot{X} = \frac{a}{\sqrt{f - c^2}}(\boldsymbol{M} \times \boldsymbol{\gamma}, \boldsymbol{\omega} - \boldsymbol{\Omega}), \quad \dot{Y} = \frac{a}{\sqrt{f - c^2}}(\boldsymbol{M} - c\boldsymbol{\gamma}, \boldsymbol{\omega} - \boldsymbol{\Omega}),$$

where $\boldsymbol{\omega}$ is expressed explicitly in terms of $\boldsymbol{M}$ and $\boldsymbol{\gamma}$ for the rubber rolling model from relation (3.2), and for the classical rolling model, from the formulae (3.3). For the rubber rolling model, in these relations we also need to set $c = 0$.

We note that in both cases (the rubber rolling model and the classical rolling model) preservation of the squared momentum $F_2 = \boldsymbol{M}^2$ leads to boundedness of the trajectories of the reduced system (3.2). Thus, *there are no trajectories in which the shell accelerates constantly.* In addition, the existence of additional integrals allows one to reduce the problem to investigating a two-dimensional Poincaré map, to single out various partial solutions and to study them. Below we consider in more detail the rubber model of a rolling shell.

4. MOTION OF THE SYSTEM FROM REST FOR THE RUBBER MODEL OF A ROLLING SHELL

Consider the system (3.2) (i.e., the rubber rolling model) on the zero level set of the integral $F_2 = \boldsymbol{M}^2 = 0$ and at constant values $\boldsymbol{\Omega} = \text{const}$, $\boldsymbol{K} = \text{const}$. It follows from $F_2 = 0$ that each component of the vector of momentum $\boldsymbol{M} = 0$ is zero.

This case can be physically realized, for example, if one begins to increase the angular velocity of the frame $\boldsymbol{\Omega}(t)$ and the gyrostatic momentum $\boldsymbol{K}(t)$ from rest ($\boldsymbol{\omega} = \boldsymbol{\Omega} = \boldsymbol{K} = 0$) to some fixed values $\boldsymbol{\Omega} = \text{const}$, $\boldsymbol{K} = \text{const}$. In this case, the value $\boldsymbol{M} = 0$ will remain unchanged, since $F_2 = \boldsymbol{M}^2$ is also a first integral if $\boldsymbol{\Omega}(t)$ and $\boldsymbol{K}(t)$ depend explicitly on time.

In this case the reduced system describes a vector field on a two-dimensional sphere:

$$\mathscr{M}_0^2 = \{(\boldsymbol{M}, \boldsymbol{\gamma}) \mid \boldsymbol{M} = 0, \boldsymbol{\gamma}^2 = 1\} \approx \mathbb{S}^2,$$

which has the form

$$\dot{\boldsymbol{\gamma}} = \boldsymbol{\gamma} \times \mathbf{A}\,(Z\boldsymbol{\gamma} - \boldsymbol{K})\,, \quad Z = \frac{(\boldsymbol{\Omega} + \mathbf{A}\boldsymbol{K}, \boldsymbol{\gamma})}{(\mathbf{A}\boldsymbol{\gamma}, \boldsymbol{\gamma})}. \tag{4.1}$$

The remaining equations of motion for defining the orientation of the frame and the trajectory of the point of contact can be represented as

$$\begin{gathered} \dot{\boldsymbol{\alpha}} = \boldsymbol{\alpha} \times \mathbf{A}\,(Z\boldsymbol{\gamma} - \boldsymbol{K})\,, \quad \dot{\boldsymbol{\beta}} = \boldsymbol{\beta} \times \mathbf{A}\,(Z\boldsymbol{\gamma} - \boldsymbol{K})\,, \\ \dot{X} = a\big(\boldsymbol{\beta}, \mathbf{A}\,(Z\boldsymbol{\gamma} - \boldsymbol{K}) - \boldsymbol{\Omega}\big), \quad \dot{Y} = -a\big(\boldsymbol{\alpha}, \mathbf{A}\,(Z\boldsymbol{\gamma} - \boldsymbol{K}) - \boldsymbol{\Omega}\big). \end{gathered} \tag{4.2}$$

Thus, at the first stage the problem reduces to investigating the two-dimensional autonomous system (4.1), in which chaotic trajectories are known to be absent.

When $\boldsymbol{\Omega} = 0$, the system (4.1) describes a particular case of generalization of the problem of the rubber Chaplygin ball with a gyrostat [8, 27] and admits the first integral

$$\frac{(\mathbf{A}\boldsymbol{K}, \boldsymbol{\gamma})^2}{(\mathbf{A}\boldsymbol{\gamma}, \boldsymbol{\gamma})} = \text{const}.$$

In the general case, the level surface of this integral is an elliptic cone, so that in this case all trajectories of the system (4.1) on the sphere $\boldsymbol{\gamma}^2 = 1$ turn out to be closed. Below it will be shown that, if $\boldsymbol{\Omega} \neq 0$, then the system (4.1) has asymptotically stable equilibrium points and limit cycles.

Remark 6. The system (4.1) possesses the symmetry $\boldsymbol{\gamma} \to -\boldsymbol{\gamma}$. As a result, isolated fixed points occur in pairs.

4.1. The Absence of Gyrostatic Momentum $\boldsymbol{K} = 0$

If $\boldsymbol{K} = 0$, then the system (4.1) has an additional integral

$$F_3 = (\mathbf{A}\boldsymbol{\gamma}, \boldsymbol{\gamma}).$$

Remark 7. According to (3.1), this case cannot be realized without gyrostatic momentum $\boldsymbol{k}$.

In this case, after rescaling time by

$$dt \to \frac{(\mathbf{A}\boldsymbol{\gamma}, \boldsymbol{\gamma})}{(\boldsymbol{\Omega}, \boldsymbol{\gamma})} dt \tag{4.3}$$

the equations of motion can be reduced to the Euler equations for the motion of a rigid body with a fixed point. Then, as is well known (see, e. g., [17]), there are six isolated fixed points on the Poisson sphere:

$$\Gamma_{1,2} = (\pm 1, 0, 0), \quad \Gamma_{3,4} = (0, \pm 1, 0), \quad \Gamma_{5,6} = (0, 0, \pm 1). \tag{4.4}$$

If none of the angular velocity components of the frame is zero $\Omega_i \neq 0$, where $i = 1, 2, 3$, then the following proposition holds for points $\Gamma_1, \ldots, \Gamma_6$.

Proposition 1. *Let $a_1 < a_2 < a_3$. Then the fixed points $\Gamma_{3,4}$ of the system (4.1) are orbitally unstable, and $\Gamma_{1,2}$ and $\Gamma_{5,6}$ are orbitally stable. They correspond to the case in which the frame rotates along the principal axis of inertia and the point of contact of the shell traces out a circle.*

Proof. The stability property follows from the Euler case in rigid body dynamics (see, e. g., [17]). We show that at the equilibrium points the shell moves in a circle, as illustrated by Γ_5.

From (4.2) we obtain

$$\boldsymbol{\alpha} = \big(\sin(\Omega_3 t + \phi_0), \cos(\Omega_3 t + \phi_0), 0\big), \quad \phi_0 = \text{const},$$
$$\boldsymbol{\beta} = \big(-\cos(\Omega_3 t + \phi_0), \sin(\Omega_3 t + \phi_0), 0\big).$$

The equations for the trajectory of the point of contact can be represented as

$$\dot{X} = a\Omega_1 \cos(\Omega_3 t + \phi_0) - a\Omega_2 \sin(\Omega_3 t + \phi_0),$$
$$\dot{Y} = a\Omega_2 \cos(\Omega_3 t + \phi_0) + a\Omega_1 \sin(\Omega_3 t + \phi_0).$$

Explicitly integrating them, we find that the point of contact moves in a circle:

$$\big(X(t) - x_0\big)^2 + \big(Y(t) - y_0\big)^2 = a^2 \frac{\Omega_1^2 + \Omega_2^2}{\Omega_3^2}, \quad x_0, y_0 = \text{const}. \qquad \square$$

In the system (4.1) we can single out the plane

$$\Sigma^1 = \{(\boldsymbol{\Omega}, \boldsymbol{\gamma}) = 0\},$$

in which the time rescaling (4.3) has a singularity. The intersection of Σ^1 with the Poisson sphere defines a circle filled by fixed points of the system (4.1): asymptotically stable Σ^1_s or asymptotically unstable Σ^1_u:

$$\Sigma^1_s = \{(\boldsymbol{\Omega}, \boldsymbol{\gamma}) = 0, (\mathbf{A}\boldsymbol{\gamma}, \boldsymbol{\gamma} \times \boldsymbol{\Omega}) > 0\},$$
$$\Sigma^1_u = \{(\boldsymbol{\Omega}, \boldsymbol{\gamma}) = 0, (\mathbf{A}\boldsymbol{\gamma}, \boldsymbol{\gamma} \times \boldsymbol{\Omega}) < 0\}.$$

At the equilibrium points Σ^1_s and Σ^1_u the frame is at rest relative to the fixed coordinate system, and the point of contact moves along a straight line.

As in the Euler case [17], the integral curves of the system ζ are an intersection of the sphere $\boldsymbol{\gamma}^2 = 1$ and the ellipsoids $\boldsymbol{F}_3 = \text{const}$. If the integral curve ζ does not intersect Σ^1, then it coincides with the periodic trajectory of the system in the Euler case. Conversely, if it intersects Σ^1, then the trajectory asymptotically tends to the equilibrium point $\Sigma^1_s \cup \zeta$. A typical view of trajectories on the Poisson sphere and of the point of contact of the shell on the plane for the case $\boldsymbol{K} = 0$ is presented in Fig. 5.

4.2. The Case $\boldsymbol{K} \neq 0$

Let the gyrostatic momentum be directed along one of the principal axes:

$$\boldsymbol{K} = (0, 0, K_3). \tag{4.5}$$

Let us consider how the trajectories of the system (4.1) behave as $|K_3|$ increases. In this case, from (4.4), at all values of K_3, only the following equilibrium points are preserved:

$$\Gamma_{5,6} = (0, 0, \pm 1). \tag{4.6}$$

Proposition 2. *Depending on the values of*

$$A_1 = a_1 a_3 K_3 + (a_1 - a_3)\Omega_3, \quad A_2 = a_2 a_3 K_3 + (a_2 - a_3)\Omega_3$$

the equilibrium points (4.6) *of the system* (4.1) *with nonzero gyrostatic momentum* (4.5) *can be of the following types: a saddle* $(A_1 A_2 < 0)$ *or a weak focus* $(A_1 A_2 > 0)$. *Depending on the value of*

$$B = K_3 \Omega_1 \Omega_2 \big((a_2 - a_3)^2 A_1^2 - (a_1 - a_3)^2 A_2^2\big),$$

the focus is:

— *stable if* $\dfrac{B}{A_1} > 0$;[4)]

— *unstable if* $\dfrac{B}{A_1} < 0$.

[4)] Since in the case of a weak focus both quantities A_1 and A_2 have the same signs, the signs of the quantities $\frac{B}{A_1}$ and $\frac{B}{A_2}$ coincide.

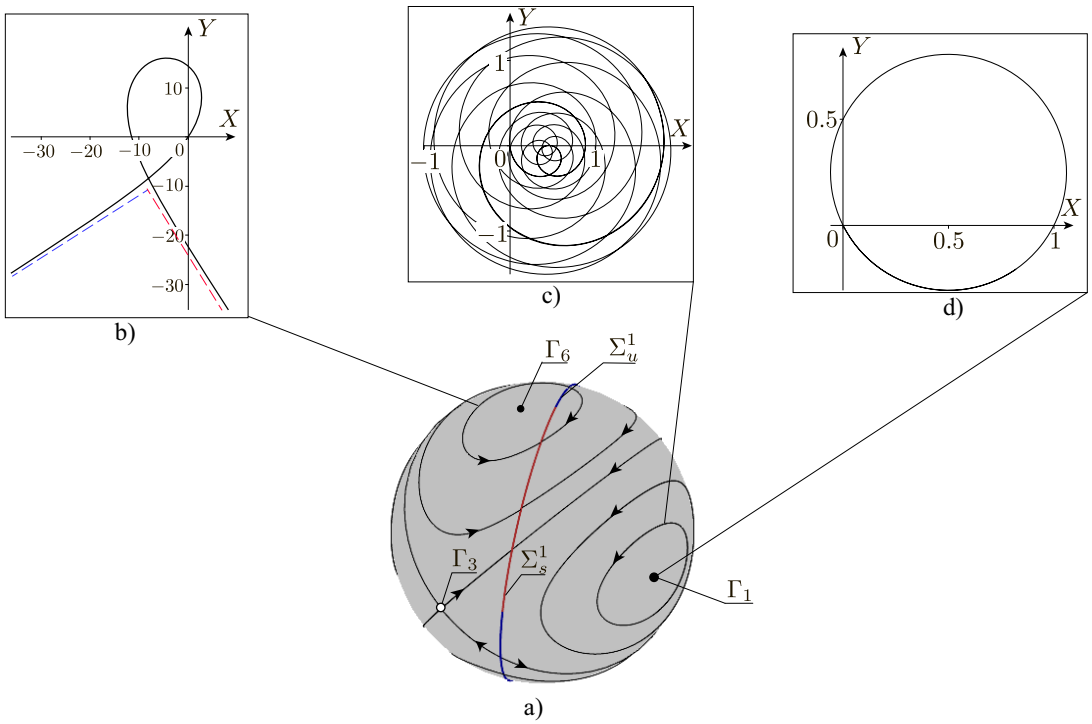

Fig. 5. A typical view of trajectories on the Poisson sphere and of the point of contact for $\boldsymbol{K} = 0$ and the fixed parameters $\boldsymbol{\Omega} = (4, 2, 1)$, $\mathbf{A} = \mathrm{diag}(0.5, 0.4, 0.3)$, $a = 1$ for the initial position of the point of contact $X(0) = 0$, $Y(0) = 0$. The initial conditions for the unit vectors are: b) $\boldsymbol{\alpha}(0) = (\frac{\sqrt{8949}}{95}, \frac{2\sqrt{19}}{95}, 0)$, $\boldsymbol{\beta}(0) = (-\frac{9\sqrt{19}}{475}, -\frac{9\sqrt{8949}}{950}, -\frac{\sqrt{19}}{10})$, $\boldsymbol{\gamma}(0) = (\frac{1}{25}, \frac{\sqrt{471}}{50}, -\frac{9}{10})$; c) $\boldsymbol{\alpha}(0) = (0, -1, 0)$, $\boldsymbol{\beta}(0) = (\frac{\sqrt{39}}{20}, 0, -\frac{19}{20})$, $\boldsymbol{\gamma}(0) = (\frac{19}{20}, 0, \frac{\sqrt{39}}{20})$; d) $\boldsymbol{\alpha}(0) = (0, -1, 0)$, $\boldsymbol{\beta}(0) = (0, 0, -1)$, $\boldsymbol{\gamma}(0) = (1, 0, 0)$.

Proof. The equations of motion in a neighborhood of Γ_6 (the analysis of the equilibrium point Γ_5 is carried out analogously) have, up to quadratic terms, the form

$$\dot\gamma_1 = -\frac{A_2}{a_3}\gamma_2 - \frac{(a_2 - a_3)\Omega_1}{a_3}\gamma_1\gamma_2 - \frac{(a_2 - a_3)\Omega_2}{a_3}\gamma_2^2,$$
$$\dot\gamma_2 = \frac{A_1}{a_3}\gamma_2 + \frac{(a_1 - a_3)\Omega_1}{a_3}\gamma_1\gamma_2 + \frac{(a_1 - a_3)\Omega_2}{a_3}\gamma_1^2.$$

As can be seen, if $A_1A_2 < 0$, then the equilibrium point under consideration is of saddle type.

If $A_1A_2 > 0$, then the definition of stability requires considering quadratic terms (since for a linear system the equilibrium point Γ_6 is of center type). For this, we define a new variable and rescale time as follows:

$$\gamma_1 = \sqrt{A_1A_2}\,\frac{x}{A_1}, \quad \gamma_2 = y, \quad t = \frac{a_3}{\sqrt{A_1A_2}}\tau.$$

The equations of motion in the new variables become

$$x' = -y - \frac{(a_2 - a_3)\Omega_1}{\sqrt{A_1A_2}}xy - \frac{(a_2 - a_3)\Omega_2}{A_2}y^2,$$
$$y' = x + \frac{(a_1 - a_3)\Omega_2}{A_1}xy + \frac{(a_1 - a_3)\Omega_1A_2}{\sqrt{A_1A_2}A_1}x^2,$$

where the prime denotes the derivative with respect to τ. In this case, the type and the stability of the equilibrium point for this system are defined by the quantity (for details, see [1, 46]):

$$L_1 = \frac{B}{A_1}.$$

If $L_1 \neq 0$, then the above-mentioned equilibrium point is a (weak) focus, which is stable if $L_1 < 0$ and unstable if $L_1 > 0$. The case $L_1 = 0$ requires a separate analysis. □

In this case, the relation $(\mathbf{\Omega}, \boldsymbol{\gamma}) = 0$ does not define the family of fixed points. However, at sufficiently small $|K_3|$ there are two types of isolated equilibrium points.

The isolated equilibrium points of the first type are

$$\Delta = \{\gamma_1 = 0,\ \gamma_2 = \sin\varphi,\ \gamma_3 = \cos\varphi\},$$
$$\delta_1 = \left\{\varphi = \frac{\arcsin(\kappa_1) - \nu_1}{2}\right\},\ \delta_2 = \left\{\varphi = \frac{\arcsin(\kappa_1) - \nu_1}{2} + \pi\right\},$$
$$\delta_3 = \left\{\varphi = -\frac{\arcsin(\kappa_1) + \nu_1}{2} + \frac{\pi}{2}\right\},\ \delta_4 = \left\{\varphi = -\frac{\arcsin(\kappa_1) + \nu_1}{2} + \frac{3\pi}{2}\right\},$$
$$\kappa_1 = \frac{(a_2 - a_3)\Omega_3 + 2a_2a_3K_3}{\sqrt{\Omega_2^2 + \Omega_3^2}(a_3 - a_2)},\ \nu_1 = \arcsin\left(\frac{\Omega_3^2}{\sqrt{\Omega_2^2 + \Omega_3^2}}\right).$$

These equilibrium points exist if $|\kappa_1| < 1$.

The isolated equilibrium points of the second type are

$$\Theta = \{\gamma_1 = \sin\varphi,\ \gamma_2 = 0,\ \gamma_3 = \cos\varphi\},$$
$$\theta_1 = \left\{\varphi = \frac{\arcsin(\kappa_2) - \nu_2}{2}\right\},\ \theta_2 = \left\{\varphi = \frac{\arcsin(\kappa_2) - \nu_2}{2} + \pi\right\},$$
$$\theta_3 = \left\{\varphi = -\frac{\arcsin(\kappa_2) + \nu_2}{+}\frac{\pi}{2}\right\},\ \theta_4 = \left\{\varphi = -\frac{\arcsin(\kappa_2) + \nu_2}{2} + \frac{3\pi}{2}\right\},$$
$$\kappa_2 = \frac{(a_1 - a_3)\Omega_3 + 2a_1a_3K_3}{\sqrt{\Omega_1^2 + \Omega_3^2}(a_3 - a_1)},\ \nu_2 = \arcsin\left(\frac{\Omega_3^2}{\sqrt{\Omega_1^2 + \Omega_3^2}}\right),$$

which exist if $|\kappa_2| < 1$.

Depending on the system parameters, the conditions for stability of these equilibrium points are represented in the form of extremely cumbersome relations. Therefore, we illustrate the evolution of the phase portrait of the system (4.1) with increasing $|K_3|$ for the fixed parameters $\mathbf{\Omega} = (4, 2, 1)$, $\mathbf{A} = \mathrm{diag}(0.5, 0.4, 0.3)$ and $a = 1$ (see Figs. 6–8).

If $0 < \kappa_2 < \kappa_1 < 1$, then on the Poisson sphere there are ten isolated fixed points of different types (see Fig. 6):

— four saddles (θ_1, θ_2, δ_3, δ_4);

— two stable foci (θ_3, θ_4);

— two unstable nodes (δ_1, δ_2);

— two slow stable foci (Γ_5, Γ_6).

We note that, in this case, the unstable and stable manifolds of equilibrium points δ_3, δ_4 and the central manifold at δ_1, δ_2 form a closed contour.

Let $\kappa_2 < 1 < \kappa_1$. Then the equilibrium points δ_1, δ_2, δ_3 and δ_4 disappear, and an unstable limit cycle arises from the closed contour (see Fig. 7). If $1 < \kappa_2 < \kappa_1$, then of all the equilibrium points the system (4.1) has only Γ_5 and Γ_6 and the unstable limit cycle (see Fig. 8).

A detailed classification of phase portraits on the Poisson sphere and of trajectories of the contact point depending on the system parameters remains an open problem.

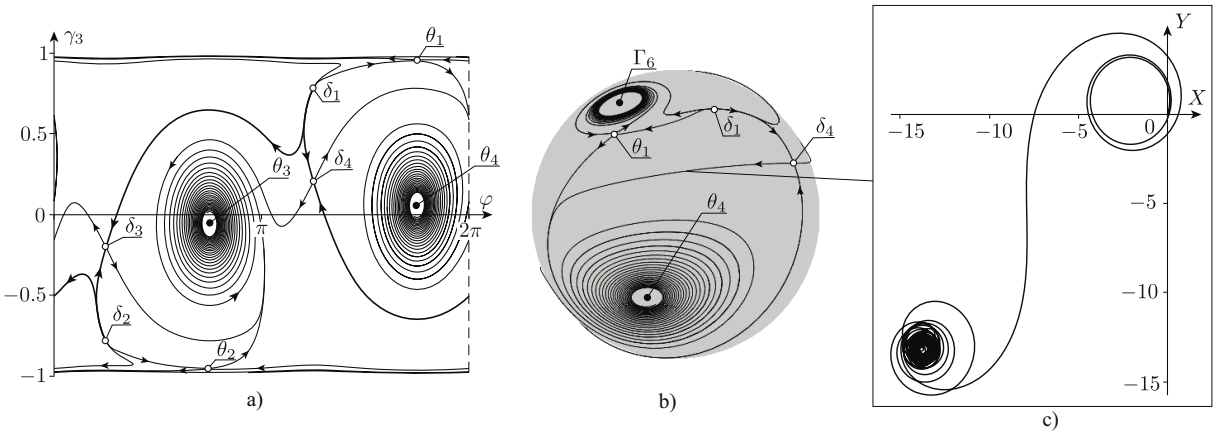

Fig. 6. Trajectories for $K_3 = 0.3$ on the Poisson sphere, its involute $\left(\varphi = \frac{\pi}{4} + \arctan\frac{\gamma_1}{\gamma_2}\right)$ and the trajectory of the contact point with the fixed initial conditions $\boldsymbol{\alpha}(0) = (1,0,0)$, $\boldsymbol{\beta}(0) = \left(0, \frac{3\sqrt{11}}{50}, -\frac{49}{50}\right)$, $\boldsymbol{\gamma}(0) = \left(0, \frac{49}{50}, \frac{3\sqrt{11}}{50}\right)$, $X(0) = 0$, $Y(0) = 0$.

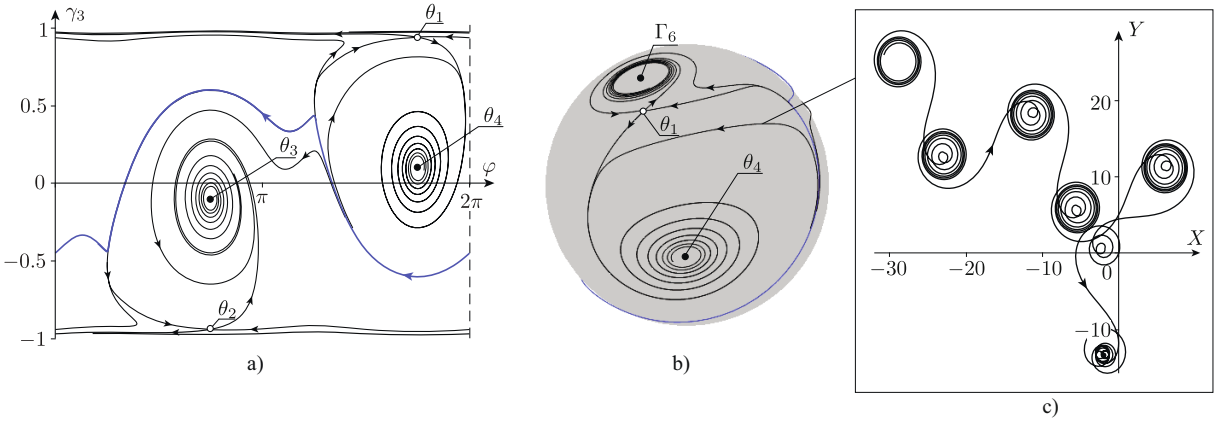

Fig. 7. Trajectories for $K_3 = 0.52$ on the Poisson sphere, its involute $\left(\varphi = \frac{\pi}{4} + \arctan\frac{\gamma_1}{\gamma_2}\right)$ and the trajectory of the contact point with the fixed initial conditions $\boldsymbol{\alpha}(0) = (1,0,0)$, $\boldsymbol{\beta}(0) = \left(0, \frac{\sqrt{79}}{40}, -\frac{39}{40}\right)$, $\boldsymbol{\gamma}(0) = \left(0, \frac{39}{40}, \frac{\sqrt{79}}{40}\right)$, $X(0) = 0$, $Y(0) = 0$. The limit cycle is shown in blue.

5. REGULAR AND CHAOTIC MOTIONS FOR THE RUBBER MODEL OF A ROLLING SHELL

5.1. Straight-line Motions

The reduced system (3.2) possesses a degenerate one-parameter family of the simplest equilibrium points for which $\boldsymbol{\omega} = 0$:

$$\Sigma^1 = \left\{\boldsymbol{M} = \boldsymbol{\gamma}_0 \times \boldsymbol{K},\ \boldsymbol{\gamma} = \boldsymbol{\gamma}_0 \mid (\boldsymbol{\Omega}, \boldsymbol{\gamma}_0) = 0,\ \boldsymbol{\gamma}_0^2 = 1\right\},\ \boldsymbol{\gamma}_0 = \text{const}. \tag{5.1}$$

In this case, the frame is at rest relative to the fixed coordinate system $OXYZ$, and the contact point P of the spherical shell traces out a straight line on the plane OXY.

Remark 8. From the viewpoint of technical and engineering applications, these solutions are of particularly great importance, since it is in this case that the stabilization of the frame (and the devices connected with it) relative to the fixed coordinate system is achieved. A similar method of gyroscopic stabilization is used in a segway, which is a frame connected with a wheel pair (instead of a spherical shell).

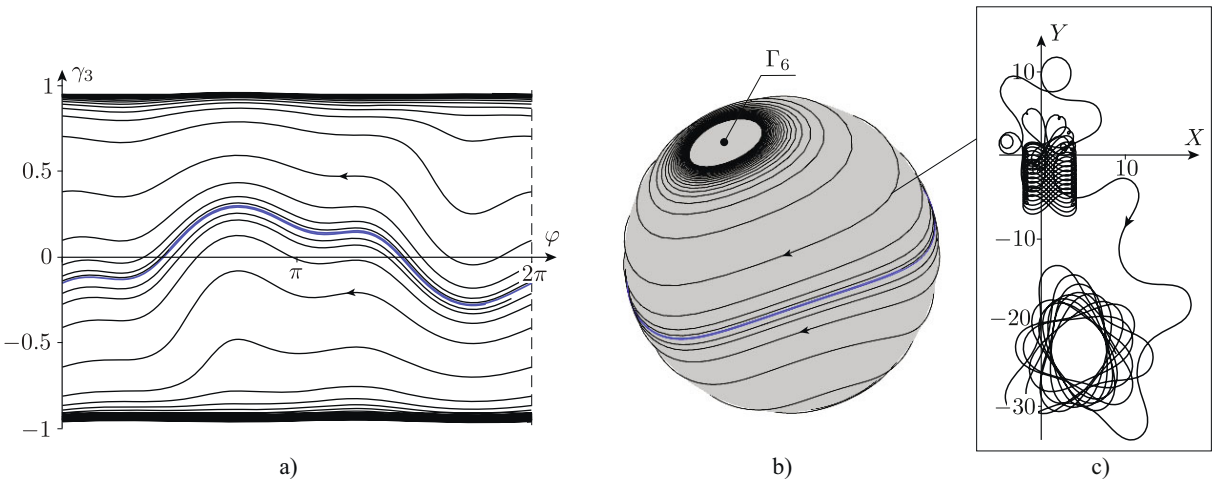

Fig. 8. Trajectories for $K_3 = 3$ on the Poisson sphere, its involute $\left(\varphi = \frac{\pi}{4} + \arctan\frac{\gamma_1}{\gamma_2}\right)$ and the trajectory of the contact point with the fixed initial conditions $\boldsymbol{\alpha}(0) = (1,0,0)$, $\boldsymbol{\beta}(0) = \left(0, \frac{\sqrt{79}}{40}, -\frac{39}{40}\right)$, $\boldsymbol{\gamma}(0) = \left(0, \frac{39}{40}, \frac{\sqrt{79}}{40}\right)$, $X(0) = 0$, $Y(0) = 0$. The limit cycle is shown in blue.

Let us analyze the stability of the found solutions. The characteristic polynomial of the linearized system (3.2) in a neighborhood of the equilibrium points Σ^1 is represented as

$$\begin{gathered} P(\lambda) = \lambda^3 P_3(\lambda), \\ P_3(\lambda) = \lambda^3 + \frac{(\mathbf{A}\boldsymbol{\gamma}_0, \boldsymbol{\gamma}_0 \times \boldsymbol{\Omega})}{(\mathbf{A}\boldsymbol{\gamma}_0, \boldsymbol{\gamma}_0)}\lambda^2 + \frac{\det \mathbf{A}}{(\mathbf{A}\boldsymbol{\gamma}_0, \boldsymbol{\gamma}_0)}\big((\boldsymbol{K}, \boldsymbol{\gamma}_0)^2 - (\boldsymbol{K}, \mathbf{A}^{-1}\boldsymbol{\Omega})\big)\lambda \\ + \frac{\det \mathbf{A}}{(\mathbf{A}\boldsymbol{\gamma}_0, \boldsymbol{\gamma}_0)}(\boldsymbol{K}, \boldsymbol{\gamma}_0)(\boldsymbol{K}, \boldsymbol{\gamma}_0 \times \boldsymbol{\Omega}). \end{gathered} \tag{5.2}$$

We see that the last term in $P_3(\lambda)$ vanishes for $\boldsymbol{K} = c\boldsymbol{\Omega}$, where $c = \text{const}$ (i.e., $\boldsymbol{K} \parallel \boldsymbol{\Omega}$). In this case, the family Σ^1 lies entirely on the fixed level set of the integral $\mathscr{M}^3_f$, $f = \boldsymbol{K}^2$. In this case, the characteristic polynomial (5.2) has the form

$$\begin{gathered} P(\lambda) = \lambda^4 P_2(\lambda), \\ P_2(\lambda) = \lambda^2 + \frac{(\mathbf{A}\boldsymbol{\gamma}_0, \boldsymbol{\gamma}_0 \times \boldsymbol{\Omega})}{(\mathbf{A}\boldsymbol{\gamma}_0, \boldsymbol{\gamma}_0)}\lambda - \frac{\det \mathbf{A}}{(\mathbf{A}\boldsymbol{\gamma}_0, \boldsymbol{\gamma}_0)}(\boldsymbol{K}, \mathbf{A}^{-1}\boldsymbol{\Omega}). \end{gathered}$$

In the general case ($\boldsymbol{K} \nparallel \boldsymbol{\Omega}$), the family Σ^1 is transverse to the level surfaces of the integrals $\mathscr{M}^3_f$. Thus, the fixed points from Σ^1 turn out to be isolated on $\mathscr{M}^3_f$. Next, we consider in detail only the case $\boldsymbol{K} \perp \boldsymbol{\Omega}$, since calculations simplify considerably in this case. A detailed analysis of all possible cases requires a separate study.

The case $\boldsymbol{K} \perp \boldsymbol{\Omega}$. The normal vector for the equilibrium points Σ^1 can be represented as

$$\boldsymbol{\gamma}_0 = c_1\boldsymbol{K} + c_2\boldsymbol{K} \times \boldsymbol{\Omega}. \tag{5.3}$$

Next, from the geometric integral and the integral $F_2 = f$ we find (taking $(\boldsymbol{\Omega}, \boldsymbol{K}) = 0$ into account):

$$\boldsymbol{K}^2(c_1^2 + c_2^2\boldsymbol{\Omega}^2) = 1,\ c_2^2\boldsymbol{K}^4\boldsymbol{\Omega}^2 = f.$$

Solving this system for the coefficients c_1 and c_2, we obtain

Proposition 3. *If $f < \boldsymbol{K}^2$, then on each level surface of the first integrals $\mathscr{M}^3_f$ there are four isolated equilibrium points Σ^1:*

$$\mathscr{M}^3_f \cap \Sigma^1 = \{\sigma_+ \cup \sigma_- \cup \delta_+ \cup \delta_-\},$$
$$\sigma_\pm = \left\{ c_1 = \pm\frac{\sqrt{\boldsymbol{K}^2 - f}}{\boldsymbol{K}^2},\ c_2 = \frac{\sqrt{f}}{\boldsymbol{K}^2\sqrt{\boldsymbol{\Omega}^2}} \right\},$$
$$\delta_\pm = \left\{ c_1 = \pm\frac{\sqrt{\boldsymbol{K}^2 - f}}{\boldsymbol{K}^2},\ c_2 = -\frac{\sqrt{f}}{\boldsymbol{K}^2\sqrt{\boldsymbol{\Omega}^2}} \right\}.$$

When $f = \boldsymbol{K}^2$, there are two of these equilibrium points and the family Σ^1 touches $\mathscr{M}^3_f$.

According to the Routh – Hurwitz criterion, for an equilibrium point to be stable, it is necessary that the free coefficient in the polynomial $P_3(\lambda)$ be positive. In this case, after substituting (5.3) into the characteristic polynomial (5.2) and after abbreviating the positive polynomial, we find the stability condition:

$$c_1 c_2 < 0.$$

This yields the following proposition.

Proposition 4. *On the fixed level set of the integrals $\mathscr{M}^3_f$, $f < \boldsymbol{K}^2$ the equilibrium points σ_+ and δ_- are unstable regardless of the parameters.*

Further, using the Routh – Hurwitz criterion, we find that, for σ_- and δ_+ to be stable, the following inequalities must be satisfied:

$$\Big(c_1\mathbf{A}\boldsymbol{K} + c_2\mathbf{A}(\boldsymbol{K}\times\boldsymbol{\Omega}), c_1\boldsymbol{\Omega}\times\boldsymbol{K} + c_2\boldsymbol{\Omega}^2\Big) > 0,$$
$$\Big(c_1\mathbf{A}\boldsymbol{K} + c_2\mathbf{A}(\boldsymbol{K}\times\boldsymbol{\Omega}), c_1\boldsymbol{\Omega}\times\boldsymbol{K} + c_2\boldsymbol{\Omega}^2\Big)\Big(c_1\boldsymbol{K}^4 - (\boldsymbol{K}, \mathbf{A}^{-1}\boldsymbol{\Omega})\Big) \tag{5.4}$$
$$+c_1c_2\boldsymbol{K}^2\Big(c_1\mathbf{A}\boldsymbol{K} + c_2\mathbf{A}(\boldsymbol{K}\times\boldsymbol{\Omega}), (c_1\boldsymbol{K} + c_2\boldsymbol{K}\times\boldsymbol{\Omega})\Big)\boldsymbol{K}^2\boldsymbol{\Omega}^2 > 0.$$

A typical view of a stability region on the parameter plane (K_1, K_2) is shown in Fig. 9.

Numerical experiments (see Fig. 10) show that, if we choose parameters in the stability region in Fig. 9, then there exist trajectories which from the neighborhood of the unstable equilibrium point (σ_+ or δ_-) tend asymptotically to another equilibrium point (σ_- or δ_+).

The trajectory of the contact point for the equilibrium points $\sigma_\pm$ and $\delta_\pm$ is described by the relations

$$X(t) = x_0, \quad Y(t) = \pm a\sqrt{\boldsymbol{\Omega}^2}t + y_0,$$
$$x_0, y_0 = \text{const},$$

where the signs + and − correspond, respectively, to $\sigma_\pm$ and $\delta_\pm$. Thus, the shell rolls along a straight line parallel to the axis OY.

5.2. Restriction of the Flow to $\mathscr{M}^3_f$ and a Poincaré Map

To carry out a numerical analysis of the behavior of the trajectories of the reduced system (3.2) in the general case, in the absence of equilibrium points Σ^1 on the integral surfaces $\mathscr{M}^3_f$ (i. e., $f > \boldsymbol{K}^2$), we use a Poincaré map.

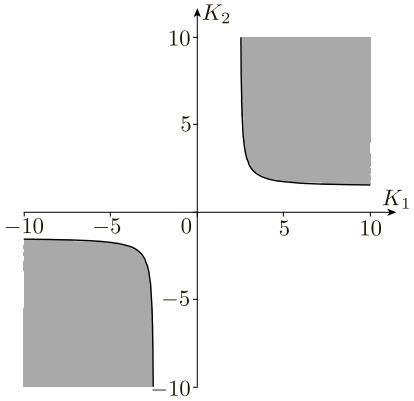

Fig. 9. The stability region (gray) of the equilibrium points σ_- and δ_+ on the parameter plane (K_1, K_2) for fixed $K_3 = 0$, $\mathbf{\Omega} = (0, 0, 1)$, $\mathbf{A} = \mathrm{diag}(0.5, 0.3, 0.6)$.

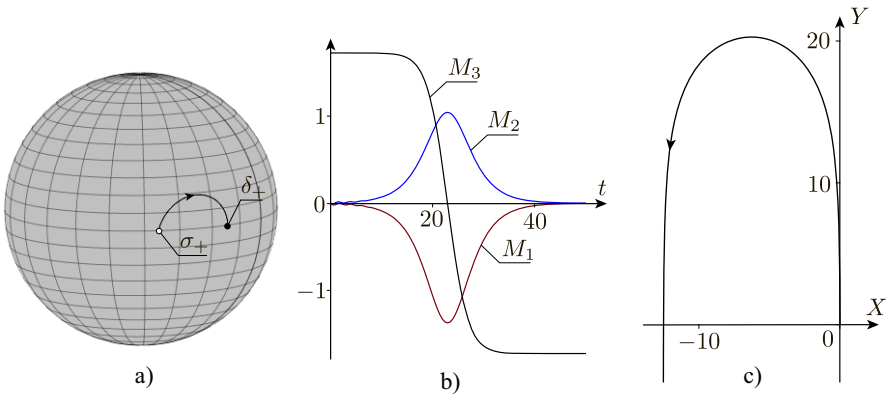

Fig. 10. Projection of the trajectory onto the Poisson sphere, the time dependence of the components of momentum $\boldsymbol{M}(t)$ and the trajectory of the contact point of the shell with the initial conditions from the neighborhood of the unstable equilibrium point σ_+ and $x(0) = 0$, $y(0) = 0$ for the fixed parameters: $\mathbf{\Omega} = (0, 0, 1)$, $\boldsymbol{K} = (4, 5, 0)$, $\mathbf{A} = \mathrm{diag}(0.5, 0.3, 0.6)$, $a = 1$, $f = 3$.

We first restrict this system to the three-dimensional manifold of the level set of the common integrals $\mathscr{M}^3_f$. For this, we use the Andoyer – Deprit variables (L, l, g) [17]:

$$\begin{gathered} M_1 = \sqrt{f - L^2}\sin l, \quad M_2 = \sqrt{f - L^2}\cos l, \quad M_3 = L, \\ \gamma_1 = \frac{L}{\sqrt{f}}\cos g \sin l + \sin g \cos l, \quad \gamma_2 = \frac{L}{\sqrt{f}}\cos g \cos l - \sin g \sin l, \\ \gamma_3 = -\sqrt{1 - \frac{L^2}{f}}\cos g, \end{gathered} \tag{5.5}$$

where $l, g \in [0, 2\pi)$ are the angle variables and L, f satisfy the obvious inequality

$$-1 \leqslant \frac{L}{\sqrt{f}} \leqslant 1.$$

As a secant for this flow on $\mathscr{M}^3_f$ we choose the submanifold given by

$$g = g_0.$$

Numerically integrating the systems under consideration and finding the intersections of trajectories with the given section, we finally obtain a family of point two-dimensional maps:

$$\begin{gathered} \Phi_{f,g_0} \colon \mathscr{M}^2_{g_0} \to \mathscr{M}^2_{g_0}, \\ \mathscr{M}^2_{g_0} = \{\boldsymbol{x} \in \mathscr{M}^3 \mid g(\boldsymbol{x}) = g_0\}. \end{gathered} \tag{5.6}$$

We will parameterize the manifold $\mathscr{M}^2_{g_0}$ by a pair of variables l mod 2π and $\frac{L}{\sqrt{f}}$ $\left(\left|\frac{L}{\sqrt{f}}\right| \leqslant 1\right)$ so that the pair $\left(l, \frac{L}{\sqrt{f}}\right)$ defines a point on the two-dimensional unit sphere S^2. The trajectories of this map for $g_0 = 0$ and different parameter values are shown in Fig. 11.

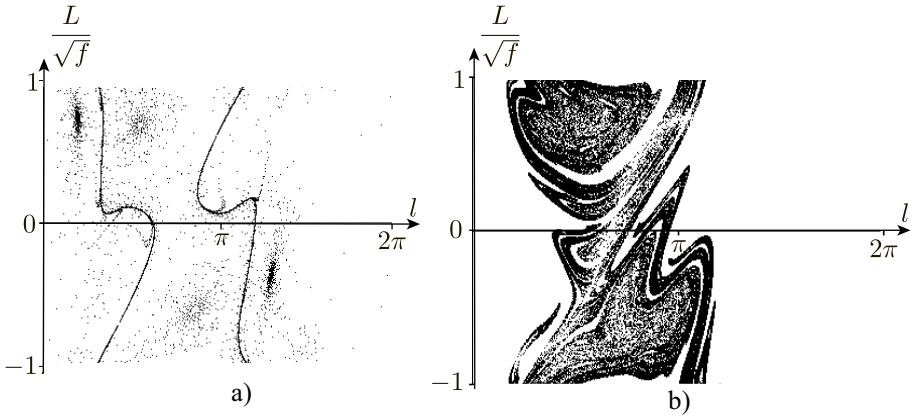

Fig. 11. A Poincaré map for the fixed parameters: a) $\boldsymbol{\Omega} = (0, 0, 2)$, $\boldsymbol{K} = (2, 2, 0)$, $\mathbf{A} = \mathrm{diag}(0.7, 0.6, 0.8)$, $f = 25$, b) $\boldsymbol{\Omega} = (0, 0, 2)$, $\boldsymbol{K} = (2, 3, 0)$, $\mathbf{A} = \mathrm{diag}(0.8, 0.6, 0.7)$, $f = 25$, $g_0 = 0$.

5.3. Asymptotically Stable Regimes of Motion (Attractors)

The numerical investigation of the Poincaré map has shown that the following types of attractors occur on it: fixed points, limit cycles and a strange (chaotic) attractor. In Fig. 11a, the fixed points Φ_{f,g_0} correspond to the largest concentration of points (almost black regions), and the limit cycle corresponds to the curve which on this involute of the sphere consists of two parts.

In $\mathscr{M}^3_f$, the fixed points of the map Φ_{f,g_0} correspond to a periodic solution and the invariant curve in Fig. 11a corresponds to a limit torus. The motion of the point of contact in this case is shown in Fig. 12b and Fig. 13b. The point of contact of the shell can be seen to undergo mean motion along the axis OX. Note that the displacement along the axis OY does not exceed some fixed value.

Moreover, a strange attractor arises at some parameters of the map Φ_{f,g_0} (see Fig. 11b). This attractor corresponds to the following Lyapunov exponents:

$$\Lambda_1 \approx 0.11, \quad \Lambda_2 \approx 0, \quad \Lambda_3 \approx 0, \quad \Lambda_4 \approx 0, \quad \Lambda_5 \approx 0, \quad \Lambda_6 \approx -0.13.$$

Its Kaplan – Yorke dimension on the Poincaré map is

$$D = 1 + \frac{\Lambda_1}{|\Lambda_6|} \approx 1.84.$$

The trajectory of the contact point for this case is shown in Fig. 14. As can be seen, the point of contact of the shell undergoes, as before, mean motion along the axis OX, but the deviation along the axis OY can increase (irregularly).

APPENDIX A. DERIVATION OF RELATIONS FOR NONHOLONOMIC CONSTRAINTS AND THE KINETIC ENERGY

In previous work (see, e. g., [41, 49]) the dynamics of systems similar to that investigated in this paper were considered in the coordinate system attached to the shell. This is due to the following fact. It is for the coordinate system of the shell that the constraint equations and the kinetic energy can be calculated in the simplest way (although the equations of motion in this coordinate system turn out to be more complicated). Therefore, in this appendix we recalculate in explicit form the constraint equation (both for the classical rolling model and for the rubber rolling model) and the

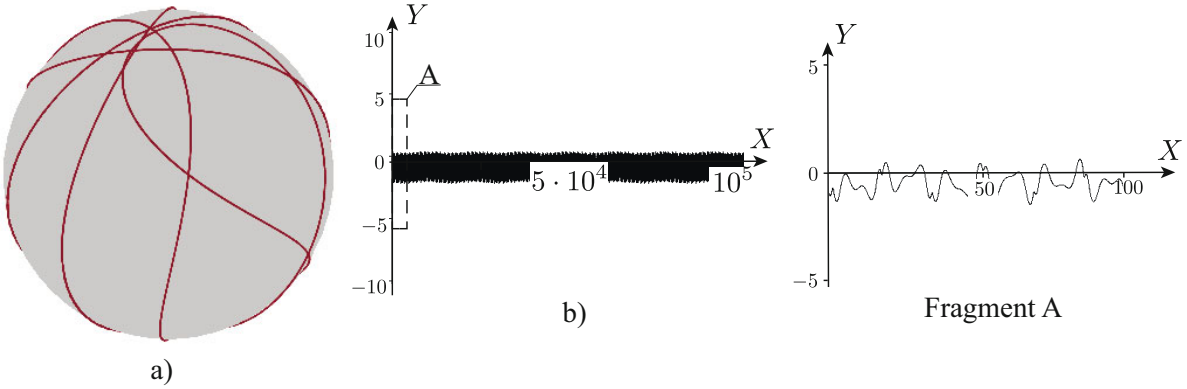

Fig. 12. Projection of the trajectory onto the Poisson sphere and the trajectory of the point of contact for the initial conditions from the neighborhood of the stable fixed point in the Poincaré map in Fig. 11a ($L = 3.6$, $l = 0.6$) and for the initial conditions $X(0) = 0$, $Y(0) = 0$, $(a = 1)$.

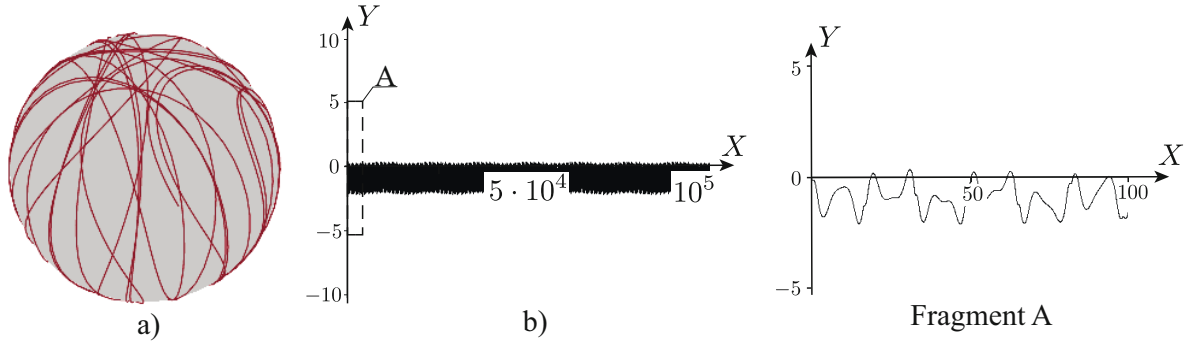

Fig. 13. Projection of the trajectory onto the Poisson sphere and the trajectory of the point of contact for the initial conditions from the neighborhood of the stable limit cycle in the Poincaré map in Fig. 11a ($L = 0$, $l = 1.96$) and for the initial conditions $X(0) = 0$, $Y(0) = 0$, $(a = 1)$.

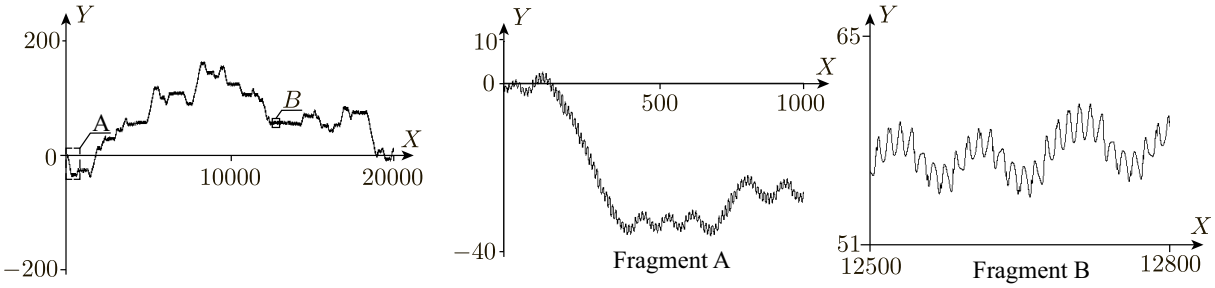

Fig. 14. The trajectory of the point of contact for the initial conditions from the neighborhood of the stable limit cycle in the Poincaré map in Fig. 11b ($L = 0$, $l = 0.6$) and for the initial conditions $X(0) = 0$, $Y(0) = 0$, $(a = 1)$.

kinetic energy to pass from the coordinate system attached to the shell to the coordinate system attached to the frame.

To specify the orientation of the shell, we introduce a *noninertial coordinate system* $Cxyz$ which is attached to the shell. We denote its unit vectors by $\boldsymbol{e}_x$, $\boldsymbol{e}_y$ and $\boldsymbol{e}_z$. Let the unit vector $\boldsymbol{e}_z = (0, 0, 1)$ be directed along the axis of dynamical symmetry of the shell. Then the angular velocity of the frame relative to the shell is defined by the relation $\Omega(t)\boldsymbol{e}_z$.

Nonholonomic constraints. Let $\boldsymbol{u}$ and $\boldsymbol{w}$ be, respectively, the translational velocity and the angular velocity of the shell, referred to the axes $Cxyz$. As is well known, the conditions that there

is no slipping and no spinning at the contact point P are defined by the following relations:

$$\boldsymbol{u} + a\boldsymbol{\Gamma} \times \boldsymbol{w} = 0, \quad (\boldsymbol{w}, \boldsymbol{\Gamma}) = 0, \tag{A.1}$$

where $\boldsymbol{\Gamma}$ is the normal to the plane projected to the axes $Cxyz$.

The rotation matrix $\mathbf{P}(t)$ which defines the transition to the coordinate system $Cx_1x_2x_3$ (attached to the frame) has the form

$$\mathbf{P}(t) = \mathbf{R}\boldsymbol{\Phi}(t),$$

$$\boldsymbol{\Phi}(t) = \begin{pmatrix} \cos\varphi(t) & \sin\varphi(t) & 0 \\ -\sin\varphi(t) & \cos\varphi(t) & 0 \\ 0 & 0 & 1 \end{pmatrix}, \quad \varphi(t) = \int_0^t \Omega(\tau)d\tau,$$

where $\mathbf{R}$ is the constant matrix.

The transition to the velocities $\boldsymbol{v}$ and $\boldsymbol{\omega}$ (in the coordinate system $Cx_1x_2x_3$) is defined by the following relations (see [17] for details):

$$\widehat{\boldsymbol{w}} = \mathbf{P}^T\widehat{\boldsymbol{\omega}}\mathbf{P} + \dot{\mathbf{P}}^T\mathbf{P}, \quad \boldsymbol{v} = \mathbf{P}\boldsymbol{u},$$
$$\widehat{\boldsymbol{\omega}} = \begin{pmatrix} 0 & \omega_3 & -\omega_2 \\ -\omega_3 & 0 & \omega_1 \\ \omega_2 & -\omega_1 & 0 \end{pmatrix}, \quad \widehat{\boldsymbol{w}} = \begin{pmatrix} 0 & w_3 & -w_2 \\ -w_3 & 0 & w_1 \\ w_2 & -w_1 & 0 \end{pmatrix}. \tag{A.2}$$

The angular velocity vector of the frame and the normal to the plane in $Cx_1x_2x_3$ have the form

$$\boldsymbol{\Omega}(t) = \Omega(t)\mathbf{P}\boldsymbol{e}_z, \quad \boldsymbol{\gamma} = \mathbf{P}\boldsymbol{\Gamma}.$$

Taking these relations into account, we represent the equations for constraints (A.1) in the form

$$\boldsymbol{v} + a\boldsymbol{\gamma} \times \big(\boldsymbol{\omega} - \boldsymbol{\Omega}(t)\big) = 0,$$
$$\big(\boldsymbol{\omega} - \boldsymbol{\Omega}(t), \boldsymbol{\gamma}\big) = 0.$$

Kinetic energy. We represent the kinetic energy of the shell as follows:

$$T_{\mathrm{s}} = \frac{1}{2}m_{\mathrm{s}}\boldsymbol{u}^2 + \frac{1}{2}(\boldsymbol{w}, \mathbf{I}_{\mathrm{s}}\boldsymbol{w}),$$

where m_{s} and $\mathbf{I}_{\mathrm{s}} = \mathrm{diag}(I_{\mathrm{s}}, I_{\mathrm{s}}, J_{\mathrm{s}})$ are the mass and the principal moments of inertia of the shell, respectively.

In the coordinate system $Cx_1x_2x_3$, up to an additive function of time, we obtain

$$T_{\mathrm{s}} = \frac{1}{2}m_{\mathrm{s}}\boldsymbol{v}^2 + \frac{1}{2}(\boldsymbol{\omega}, \mathbf{R}\mathbf{I}_{\mathrm{s}}\mathbf{R}^T\boldsymbol{\omega}) - J_{\mathrm{s}}(\boldsymbol{\omega}, \boldsymbol{\Omega}(t)).$$

The kinetic energy of the frame in the coordinate system $Cx_1x_2x_3$ can be represented as

$$T_{\mathrm{f}} = \frac{1}{2}m_{\mathrm{f}}\boldsymbol{v}^2 + \frac{1}{2}(\boldsymbol{\omega}, \mathbf{I}_{\mathrm{f}}\boldsymbol{\omega}),$$

where m_{f} and $\mathbf{I}_{\mathrm{f}}$ are the mass and the tensor of inertia of the frame, respectively.

The kinetic energy of the ith rotor has the form

$$T_i = \frac{1}{2}\mu_i\boldsymbol{v}^2 + \frac{1}{2}\big(\boldsymbol{\omega} + \dot{\phi}_i(t)\boldsymbol{n}_i, \mathbf{j}_i(\boldsymbol{\omega} + \dot{\phi}_i(t)\boldsymbol{n}_i)\big),$$

where m_i and $\mathbf{j}_i$ are the mass and the tensor of inertia of the ith rotor, respectively, and $\boldsymbol{n}_i$ is the unit vector defining its direction of rotation.

Using the fact that the axis of rotation of the rotor coincides with the axis of dynamical symmetry, i.e., $\mathbf{j}_i\boldsymbol{n}_i = j_i\boldsymbol{n}_i$, we obtain the kinetic energy of the system in the form

$$T = T_{\mathrm{s}} + T_{\mathrm{f}} + \sum_{i=1}^{n} T_i = \frac{1}{2}m\boldsymbol{v}^2 + \frac{1}{2}(\boldsymbol{\omega}, \mathbf{I}\boldsymbol{\omega}) + (\boldsymbol{k}(t), \boldsymbol{\omega}),$$

where m is the mass of the entire system, and $\mathbf{I}$ and $\boldsymbol{k}(t)$ are its moment of inertia and gyrostatic momentum, respectively:

$$\begin{gathered} m = m_{\mathrm{s}} + m_{\mathrm{f}} + \sum_{i=1}^{n} \mu_i, \quad \mathbf{I} = \mathbf{R}\mathbf{I}_{\mathrm{s}}\mathbf{R}^T + \mathbf{I}_{\mathrm{f}} + \sum_{i=1}^{n} \mathbf{j}_i, \\ \boldsymbol{k}(t) = \sum_{i=1}^{n} j_i\dot{\phi}_i(t)\boldsymbol{n}_i - J_{\mathrm{s}}\boldsymbol{\Omega}(t). \end{gathered} \tag{A.3}$$

Since the matrix $\mathbf{I}$ is symmetric and positive definite, one can always choose the matrix $\mathbf{R}$ in such a way that $\mathbf{I} = \mathrm{diag}(I_1, I_2, I_3)$ is a diagonal matrix.

FUNDING

The work of I. A. Bizyaev (Section 2 and Section 4) was supported by the Russian Science Foundation (project 18-71-00110). The work of A. V. Borisov and I. S. Mamaev was supported by the RFBR Grant No. 18-29-10051 mk and was carried out at MIPT under project 5-100 for state support for leading universities of the Russian Federation. The work of A. V. Borisov (Section 1 and Appendix A) was supported by the Russian Science Foundation (project 15-12-20035).

CONFLICT OF INTEREST

The authors declare that they have no conflicts of interest.

REFERENCES

1. Artes, J. C., Llibre, J., and Schlomiuk, D., The Geometry of Quadratic Differential Systems with a Weak Focus of Second Order, *Internat. J. Bifur. Chaos Appl. Sci. Engrg.,* 2006, vol. 16, no. 11, pp. 3127–3194.
2. Balseiro, P. and García-Naranjo, L. C., Gauge Transformations, Twisted Poisson Brackets and Hamiltonization of Nonholonomic Systems, *Arch. Ration. Mech. Anal.,* 2012, vol. 205, no. 1, pp. 267–310.
3. Bizyaev, I. A., Borisov, A. V., and Mamaev, I. S., Dynamics of the Chaplygin Ball on a Rotating Plane, *Russ. J. Math. Phys.,* 2018, vol. 25, no. 4, pp. 423–433.
4. Bizyaev, I. A., Borisov, A. V., Kozlov, V. V., and Mamaev, I. S., Fermi-Like Acceleration and Power-Law Energy Growth in Nonholonomic Systems, *Nonlinearity,* 2019, vol. 32, no. 9, pp. 3209–3233.
5. Bizyaev, I. A., Borisov, A. V., and Mamaev, I. S., Exotic Dynamics of Nonholonomic Roller Racer with Periodic Control, *Regul. Chaotic Dyn.,* 2018, vol. 23, nos. 7–8, pp. 983–994.
6. Bizyaev, I. A., Borisov, A. V., and Mamaev, I. S., The Chaplygin Sleigh with Parametric Excitation: Chaotic Dynamics and Nonholonomic Acceleration, *Regul. Chaotic Dyn.,* 2017, vol. 22, no. 8, pp. 955–975.
7. Bolotin, S. V., The Problem of Optimal Control of a Chaplygin Ball by Internal Rotors, *Regul. Chaotic Dyn.,* 2012, vol. 17, no. 6, pp. 559–570.
8. Bolsinov, A. V., Borisov, A. V., and Mamaev, I. S., Geometrisation of Chaplygin's Reducing Multiplier Theorem, *Nonlinearity,* 2015, vol. 28, no. 7, pp. 2307–2318.
9. Borisov, A. V. and Fedorov, Yu. N., On Two Modified Integrable Problems in Dynamics, *Mosc. Univ. Mech. Bull.,* 1995, vol. 50, no. 6, pp. 16–18; see also: *Vestnik Moskov. Univ. Ser. 1. Mat. Mekh.,* 1995, no. 6, pp. 102–105.
10. Borisov, A. V., Fedorov, Yu. N., and Mamaev, I. S., Chaplygin Ball over a Fixed Sphere: An Explicit Integration, *Regul. Chaotic Dyn.,* 2008, vol. 13, no. 6, pp. 557–571.
11. Borisov, A. V., Ivanova, T. B., Kilin, A. A., and Mamaev, I. S. Nonholonomic Rolling of a Ball on the Surface of a Rotating Cone, *Nonlinear Dynam.,* 2019, vol. 97, no. 2, pp. 1635–1648.
12. Borisov, A. V., Kilin, A. A., Karavaev, Y. L., and Klekovkin, A. V., Stabilization of the Motion of a Spherical Robot Using Feedbacks, *Appl. Math. Model.,* 2019, vol. 69, pp. 583–592.
13. Borisov, A. V., Kilin, A. A., and Mamaev, I. S., The Problem of Drift and Recurrence for the Rolling Chaplygin Ball, *Regul. Chaotic Dyn.,* 2013, vol. 18, no. 6, pp. 832–859.

14. Borisov, A. V., Kilin, A. A., and Mamaev, I. S., Generalized Chaplygin's Transformation and Explicit Integration of a System with a Spherical Support, *Regul. Chaotic Dyn.,* 2012, vol. 17, no. 2, pp. 170–190.
15. Borisov, A. V., Kilin, A. A., and Mamaev, I. S., How to Control Chaplygin's Sphere Using Rotors, *Regul. Chaotic Dyn.,* 2012, vol. 17, nos. 3–4, pp. 258–272.
16. Borisov, A. V. and Mamaev, I. S., Two Non-holonomic Integrable Problems Tracing Back to Chaplygin, *Regul. Chaotic Dyn.,* 2012, vol. 17, no. 2, pp. 191–198.
17. Borisov, A. V. and Mamaev, I. S., *Rigid Body Dynamics,* De Gruyter Stud. Math. Phys., vol. 52, Berlin: De Gruyter, 2018.
18. Borisov, A. V. and Mamaev, I. S., Symmetries and Reduction in Nonholonomic Mechanics, *Regul. Chaotic Dyn.,* 2015, vol. 20, no. 5, pp. 553–604.
19. Borisov, A. V. and Mamaev, I. S., Conservation Laws, Hierarchy of Dynamics and Explicit Integration of Nonholonomic Systems, *Regul. Chaotic Dyn.,* 2008, vol. 13, no. 5, pp. 443–490.
20. Borisov, A. V. and Mamaev, I. S., The Rolling Motion of a Rigid Body on a Plane and a Sphere: Hierarchy of Dynamics, *Regul. Chaotic Dyn.,* 2002, vol. 7, no. 2, pp. 177–200.
21. Borisov, A. V. and Mamaev, I. S., The Dynamics of the Chaplygin Ball with a Fluid-Filled Cavity, *Regul. Chaotic Dyn.,* 2013, vol. 18, no. 5, pp. 490–496.
22. Borisov, A. V. and Mamaev, I. S., Obstacle to the Reduction of Nonholonomic Systems to the Hamiltonian Form, *Dokl. Phys.,* 2002, vol. 47, no. 12, pp. 892–894; see also: *Dokl. Akad. Nauk,* 2002, vol. 387, no. 6, pp. 764–766.
23. Borisov, A. V. and Mamaev, I. S., Chaplygin's Ball Rolling Problem Is Hamiltonian, *Math. Notes,* 2001, vol. 70, nos. 5–6, pp. 720–723; see also: *Mat. Zametki,* 2001, vol. 70, no. 5, pp. 793–795.
24. Borisov, A. V., Mamaev, I. S., and Bizyaev, I. A., Dynamical Systems with Non-Integrable Constraints: Vaconomic Mechanics, Sub-Riemannian Geometry, and Non-Holonomic Mechanics, *Russian Math. Surveys,* 2017, vol. 72, no. 1, pp. 1–32; see also: *Uspekhi Mat. Nauk,* 2017, vol. 72, no. 5(437), pp. 3–62.
25. Borisov, A. V., Mamaev, I. S., and Bizyaev, I. A., Historical and Critical Review of the Development of Nonholonomic Mechanics: the Classical Period, *Regul. Chaotic Dyn.,* 2016, vol. 21, no. 4, pp. 455–476.
26. Borisov, A. V., Mamaev, I. S., and Bizyaev, I. A., The Jacobi Integral in Nonholonomic Mechanics, *Regul. Chaotic Dyn.,* 2015, vol. 20, no. 3, pp. 383–400.
27. Borisov, A. V., Mamaev, I. S., and Bizyaev, I. A., The Hierarchy of Dynamics of a Rigid Body Rolling without Slipping and Spinning on a Plane and a Sphere, *Regul. Chaotic Dyn.,* 2013, vol. 18, no. 3, pp. 277–328.
28. Borisov, A. V., Mamaev, I. S., and Kilin, A. A., The Rolling Motion of a Ball on a Surface. New Integrals and Hierarchy of Dynamics, *Regul. Chaotic Dyn.,* 2002, vol. 7, no. 2, pp. 201–219.
29. Chaplygin, S. A., On a Ball's Rolling on a Horizontal Plane, *Regul. Chaotic Dyn.,* 2002, vol. 7, no. 2, pp. 131–148; see also: *Math. Sb.,* 1903, vol. 24, no. 1, pp. 139–168.
30. Chaplygin, S. A., On the Theory of Motion of Nonholonomic Systems. The Reducing-Multiplier Theorem, *Regul. Chaotic Dyn.,* 2008, vol. 13, no. 4, pp. 369–376.
31. Chaplygin, S. A., On Some Generalization of the Area Theorem with Applications to the Problem of Rolling Balls, *Regul. Chaotic Dyn.,* 2012, vol. 17, no. 2, pp. 199–217.
32. Chaplygin, S. A., On a Pulsating Cylindrical Vortex, *Regul. Chaotic Dyn.,* 2007, vol. 12, no. 1, pp. 101–116.
33. Chaplygin, S. A., One Case of Vortex Motion in Fluid, *Regul. Chaotic Dyn.,* 2007, vol. 12, no. 2, pp. 219–232.
34. Ehlers, K. M. and Koiller, J., Rubber Rolling: Geometry and Dynamics of $2-3-5$ Distributions, in *Proc. IUTAM Symposium 2006 on Hamiltonian Dynamics, Vortex Structures, Turbulence (Moscow, Russia, 25–30 August 2006),* pp. 469–480.
35. Fassò, F., García-Naranjo, L. C., and Sansonetto, N., Moving Energies As First Integrals of Nonholonomic Systems with Affine Constraints, *Nonlinearity,* 2018, vol. 31, no. 3, pp. 755–782.
36. Fassò, F. and Sansonetto, N., Conservation of "Moving" Energy in Nonholonomic Systems with Affine Constraints and Integrability of Spheres on Rotating Surfaces, *J. Nonlinear Sci.,* 2016, vol. 26, no. 2, pp. 519–544.
37. Fedorov, Yu. N., Motion of a Rigid Body in a Spherical Suspension, *Vestn. Mosk. Univ. Ser. 1. Mat. Mekh.,* 1988, no. 5, pp. 91–93 (Russian).
38. Fedorov, Y. N. and Kozlov, V. V., Various Aspects of n-Dimensional Rigid Body Dynamics, *Amer. Math. Soc. Transl. (2),* 1995, vol. 168, pp. 141–171.
39. Golubev, V. V., *Chaplygin,* Izhevsk: Institute of Computer Science, 2002 (Russian).
40. Hatcher, A., *Algebraic Topology,* Cambridge: Cambridge Univ. Press, 2002.
41. Ilin, K. I., Moffatt, H. K., and Vladimirov, V. A., Dynamics of a Rolling Robot, *Proc. Natl. Acad. Sci. USA,* 2017, vol. 114, no. 49, pp. 12858–12863.
42. Kilin, A. A., Pivovarova E. N., Qualitative Analysis of the Nonholonomic Rolling of a Rubber Wheel with Sharp Edges, *Regul. Chaotic Dyn.,* 2019, vol. 24, no. 2, pp. 212–233.

43. Kilin, A. A. and Pivovarova, E. N., Chaplygin Top with a Periodic Gyrostatic Moment, *Rus. J. Math. Phys.,* 2018, vol. 25, no. 4, pp. 509–524.
44. Kozlov, V. V., On the Theory of Integration of the Equations of Nonholonomic Mechanics, *Regul. Chaotic Dyn.,* 2002, vol. 7, no. 2, pp. 191–176.
45. Kuleshov, A. S., On the Generalized Chaplygin Integral, *Regul. Chaotic Dyn.,* 2001, vol. 6, no. 2, pp. 227–232.
46. Li, C., Two Problems of Planar Quadratic Systems, *Sci. Sinica Ser. A,* 1983, vol. 26, no. 5, pp. 471–481.
47. Lichtenberg, A. J., Lieberman, M. A., and Cohen, R. H., Fermi Acceleration Revisited, *Phys. D,* 1980, vol. 1, no. 3, pp. 291–305.
48. Markeev, A. P., Integrability of the Problem of Rolling of a Sphere with a Multiply Connected Cavity Filled with an Ideal Fluid, *Izv. Akad. Nauk SSSR. Mekh. Tverd. Tela,* 1986, vol. 21, no. 1, pp. 64–65 (Russian).
49. Putkaradze, V. and Rogers, S., On the Dynamics of a Rolling Ball Actuated by Internal Point Masses, *Meccanica,* 2018, vol. 53, no. 15, pp. 3839–3868.
50. Svinin, M., Morinaga, A., and Yamamoto, M., On the Dynamic Model and Motion Planning for a Spherical Rolling Robot Actuated by Orthogonal Internal Rotors, *Regul. Chaotic Dyn.,* 2013, vol. 18, nos. 1–2, pp. 126–143.
51. Tsiganov, A. V., Hamiltonization and Separation of Variables for a Chaplygin Ball on a Rotating Plane, *Regul. Chaotic Dyn.,* 2019, vol. 24, no. 2, pp. 171–186.
52. Tsiganov, A. V., On the Poisson Structures for the Nonholonomic Chaplygin and Veselova Problems, *Regul. Chaotic Dyn.,* 2012, vol. 17, no. 5, pp. 439–450.